Revealing the pace of river landscape evolution during the Quaternary: recent developments in numerical dating methods

Gilles Rixhon, Rebecca M. Briant, Stéphane Cordier, Mathieu Duval, Anna Jones, Denis Scholz

Abstract

During the last twenty years, several technical developments have considerably intensified the use of numerical dating methods for the Quaternary. The study of fluvial archives has greatly benefited from these enhancements, opening new dating horizons for a range of archives at distinct time scales and thereby providing new insights into previously unanswered questions. In this contribution, we separately present the state of the art of five numerical dating methods that are frequently used in the fluvial context: radiocarbon, Luminescence, Electron Spin Resonance (ESR), ^{230}Th/U and terrestrial cosmogenic nuclides (TCN) dating. We focus on the major recent developments for each technique that are most relevant for new dating applications in diverse fluvial environments and on explaining these for non-specialists. Therefore, essential information and precautions about sampling strategies in the field and/or laboratory procedures are provided. For each method, new and important implications for chronological reconstructions of Quaternary fluvial landscapes are discussed and, where necessary, exemplified by key case studies. A clear statement of the current technical limitations of these methods is included and forthcoming developments, which might possibly open new horizons for dating fluvial archives in the near future, are summarised.

Keywords: numerical dating method, fluvial archives, Quaternary, ^{14}C dating, Luminescence dating, ESR dating, ^{230}Th/U dating, terrestrial cosmogenic nuclides dating

1. Introduction

Unravelling processes and rates of long-term landscape evolution, focusing on the evolution of river drainage systems, has been a core topic in the earth surface sciences since Davis's (1899) pioneering work more than a century ago. Since then, river terrace sequences and/or related landforms have thus

been extensively used as geomorphic markers across the world. However, assigning chronologies to these sequences and related river sediments or landforms has constantly been challenging. Until the late 20th century, this goal was often achieved using diverse methods that provide relative age information on Quaternary fluvial deposits. Such methods included: correlation with the alpine glacial chronology (e.g. Brunnacker et al., 1982), soil chronosequences (e.g. Engel et al., 1996), palaeomagnetism (e.g. Jacobson et al., 1988), clast seismic velocity (e.g. Crook, 1986), weathering rind analysis (e.g. Colman & Pierce, 1981), obsidian hydration (e.g. Adams et al., 1992), amino-acid racemization of terrestrial molluscs (e.g. Bates, 1994) or correlation to Marine Isotope Stages (MIS) via mammalian (e.g. Schreve, 2001) and molluscan (e.g. Preece, 1999) biostratigraphy. Combining these methods often yielded insightful relative chronologies for Quaternary terrace flights (e.g. Knuepfer, 1988; Schreve et al., 2007).

Whilst methodological improvements to some of these techniques have since been achieved (e.g. Penkman et al., 2007 for amino-acid racemization), in most instances, relative dating methods have been progressively supplemented by dating methods delivering absolute numerical ages over the last two or three decades. With the exception of radiocarbon dating, which has been applied since Libby's seminal paper (Libby et al., 1949), the development of most of these geochronometers occurred in relation to major theoretical and/or technical improvements in the late 20th century. For instance, although cosmic rays were discovered in 1912 by the Nobel laureate Victor Hess, only the development of accelerator mass spectrometers (AMS) in the 1980s enabled measurements of cosmogenic nuclide concentrations (e.g. Klein et al., 1982) and thus their use as a geochronometer (e.g. Nishiizumi et al., 1986). Likewise, Electron Spin Resonance (ESR) spectroscopy, already outlined in the mid 1930s (Gorter, 1936), was first successfully applied as a dating tool only 40 years later (Ikeya, 1975).

In the framework of this FLAG (Fluvial Archives Goup) special issue, we present and discuss the recent major dating advances offered by modern numerical methods in diverse fluvial environments. Five methods are discussed: radiocarbon, Luminescence, Electron Spin Resonance, ^{230}Th/U and terrestrial cosmogenic nuclide (TCN) dating. They were specifically selected amongst the array of Quaternary dating methods because (i) they are commonly used in the fluvial context, (ii) they have all experienced major theoretical and/or technical developments during recent decades, (iii) they require different dateable material and thereby may also yield information about a wide range of fluvial processes and environments, (iv) they have different time ranges of application, but altogether, span

the last million years (Fig. 1). Detailing all theoretical principles of the individual techniques is beyond the scope of this contribution. Instead, the focus is on relevant major technical developments and how these enabled new dating applications for different kinds of fluvial archives in distinct settings. The pathways of dateable material within fluvial systems are detailed in Figure 2. Fundamental information and precautions about sampling strategies in the field and/or laboratory procedures are also provided. Whilst these are well known by geochronologists, they have not often been published and need therefore to be clarified to non-specialists who intent to collect samples for dating. For each method, new and important implications for chronological reconstructions of Quaternary fluvial landscapes are also discussed and, if necessary, exemplified. Case studies published in outputs related to former FLAG activities and using one (or more) of these dating method(s) are listed in Table 1. Current technical limitations and probable forthcoming developments are also addressed.

2. Radiocarbon dating of fluvial deposits

Radiocarbon dating has been a common method applied to fluvial deposits in those settings where organic material is readily preserved within sequences, i.e. partially or fully waterlogged parts of the floodplain system, including channels and overbank deposits (Fig. 2). As a technique it has contributed significantly to understanding key questions, both about palaeoenvironmental information contained within fluvial deposits (e.g. Kasse et al., 1995) and about periods of river activity (e.g. Macklin et al., 2005). The accuracy with which age estimates can be gained from ever smaller samples has improved significantly over the 60-70 years since the first development of the technique. This is partly due to the increasingly routine use of accelerator mass spectrometry (AMS) measurements of smaller samples (~1 mg in some cases, Ruff et al., 2010, but more robustly 5-6 mg, Brock et al., 2010). Another important development has been the significant international cooperation involved in calibrating radiocarbon measurements against independent annually-resolved records to account for natural variability in the concentration of atmospheric ^{14}C, culminating most recently in the IntCal13 dataset (Reimer et al., 2013).

The ^{14}C dating method can be applied to any material that contains carbon. This includes: cellulose-containing materials (wood, seeds, plant remains), charcoal and charred material, carbonates (including corals, foraminifera, shells), collagen-containing materials (bone, tooth, antler, ivory), hair, and bulk sediment. Many of these are found within fluvial deposits in more temperate environments, where preservation conditions are favourable, but not all are *in situ* (Fig. 2). Therefore, when

considering the radiocarbon dating of fluvial deposits, we need to consider the issue of provenance and reworking. In addition, calibration, reservoir effects and appropriate pretreatments are also relevant to fluvial archives in lakes, but reviewed elsewhere (Brauer et al., 2014).

All present-day carbon-bearing material contains three naturally occurring carbon isotopes. Of these, ^{14}C is radioactive, with a half life of 5730 ± 40 years (Godwin, 1962). The source of this ^{14}C is cosmic ray activity in the atmosphere. This enters the global carbon cycle when it is oxidised to CO_2, and concentrations are very low compared to ^{12}C and ^{13}C. Conventional radiocarbon ages are calculated from measured concentrations of ^{14}C, using either beta counting methods or, meanwhile more commonly, AMS. To allow consistency with earlier analyses, these are reported using the original Libby half life of 5568 years (e.g. Stuiver and Polach, 1977; Reimer et al., 2004). They are also corrected for fractionation processes that occur during measurement, as described by Brauer et al. (2014). Because of the multiple stages at which differences can occur within the calculation of a radiocarbon age, they should be reported in detail according to the conventions described by Millard (2014).

2.1. Provenance and reworking of radiocarbon samples in the fluvial environment

A feature of fluvial systems is the wide range of depositional environments which may be found within a single catchment, including, for instance, river channel, floodplain and floodbasin deposits. These differ in frequency of depositional events, deposited grain sizes and likely presence of *in situ* organics (Fig. 2). The nature and rate of fluvial activity within a reach determine the spatial distribution of depositional environments and their preservation within the alluvial record (Lewin and Macklin, 2003). The depositional context of a radiocarbon-dated sample determines its suitability for answering questions about the timing of events within a fluvial system. Where possible, a distinction should therefore be made between radiocarbon dates from within thick sedimentary units and those collected at or close to boundaries between units. The former provide a single age for processes, such as vertical sediment accretion or lateral channel migration, operating over an extended time period (Lewin et al., 2005), while the latter constrain the timing of events in the river system that produced sedimentological changes (Macklin and Lewin, 2003). In Late Pleistocene to Holocene settings, where detailed sedimentological information is more commonly preserved, radiocarbon dates on fluvial units have been classified as river activity ages, in minerogenic sediment, or river stability ages, on peat or palaeosols (Zielhofer and Faust, 2008). Sedimentary units indicative of river activity and river stability

may be produced simultaneously in different depositional environments within a single reach (Zielhofer and Faust, 2008). Radiocarbon dates close to sediment unit boundaries provide maximum or minimum ages for events which produced features such as reversals in fining upwards sediment sequences or renewed fluvial sedimentation above a peat or palaeosol (Macklin et al., 2005). Radiocarbon-dated samples from a unit directly below such a sedimentological change, giving a maximum age ('change after' dates), are regarded as the most reliable indicator of the age of the event which produced the change in sedimentation rate or grain size (Macklin et al., 2010). In older deposits, where fewer units are amenable to radiocarbon dating, such precise analysis of how the dates relate to fluvial activity is less feasible. Nonetheless, the sedimentological setting should be assessed in a similar way so that the age estimate obtained can be most effectively interpreted. In addition, care should be taken to interpret the different transport pathways of the type of material to be dated.

Further to their diversity, river catchment systems are highly dynamic and material can be transported varying distances from the original source. It can also be kept in storage on hillslopes or within floodplains and released into the channel tens to thousands of years afterwards (Fig. 2). Therefore, when radiocarbon dating material from fluvial deposits, the possibility of reworking must always be borne in mind. This can be especially problematic in relation to carbon-bearing material that does not easily break down in transport (Fig. 2), for example wood, bone and some shells (either because they are calcitic, such as shell opercula, or because they are light and travel in suspension rather than bedload). Therefore, it is essential to date only the identifiable fraction of the deposit (Table 2). In addition to being identifiable, it is necessary to exercise common sense over how likely the material isolated is to have been contemporaneous with deposition (e.g. not choosing material suggesting a temperate climate if preserved within cold stage deposits).

2.2. Calibration

Due to natural variability in cosmic ray production and exchange between different carbon stores (i.e. ocean, terrestrial ecosystems and atmosphere) the concentration of ^{14}C in the atmosphere varies over time. For this reason, to convert radiocarbon ages to calendar ages, a detailed calibration curve has been constructed from independently dated (often annually resolved) records including tree-rings, varves, corals and speleothems. The tree-ring curve extends to 13,900 cal years BP (Reimer et al., 2013) and is the most robust part of the curve. The extension beyond this to 50,000 cal years BP is

based on multiple datasets which diverge from each other in places, creating larger errors. The radiocarbon community meets regularly to review this curve and the most recent data set is IntCal13 (Reimer et al., 2013) – or SHCal13 for the Southern Hemisphere (Hogg et al., 2013), which is now included in all calibration software (e.g., CALIB, OxCal, BCal). The output of calibration is an interval of possible calendar ages that correspond to the ^{14}C age calculated from the measured ^{14}C concentration. Often multiple intervals correspond to the measured concentration.

2.3. Freshwater reservoir effects and radiocarbon dating of fluvial archives

When dating plant or shell material, the preferred habitat of the species used is crucial. If the material to be dated is from an aquatic species, the chemistry of the water body must be taken into account. The presence of 'old carbon' which is 'dead' with respect to radiocarbon can lead the ^{14}C of the water to have an apparent age. This apparent age is then transferred to the material being dated. This issue has been known for many years, with very early studies showing that *Potamageton*, an aquatic plant which is believed to photosynthesise within the water column, yielded an apparent age in modern hardwater lakes of ~2000 years (Deevey et al., 1954). For this reason, the first choice of material to date would instead be a plant which photosynthesises directly with the atmosphere such as *Scirpus* or *Carex* (Deevey et al., 1954).

Determining the freshwater reservoir effect in lakes (where some fluvial archives are found) is based on the assumption that the effect has remained constant and can be corrected for. In relation to rivers, this is more problematic because most studies (e.g. Deevey et al., 1954) have been carried out in lakes. A recent study (Philippsen, 2013) of water, plants and animals from rivers in northern Germany showed significant temporal variability in the scale of reservoir age in both the dissolved inorganic carbon (DIC) from river water itself (a range of 1527-3044 years) and the reservoir age in aquatic plants (a range of 350-2690 years). Of particular interest is the finding that the radiocarbon values from river water are directly related to the balance between groundwater and precipitation inputs to the system. When precipitation was higher before samples were taken, associated radiocarbon reservoir ages of river water were younger. This means that the freshwater reservoir effect in fluvial deposits is likely to be present, but to varying degrees. The main way to avoid this issue is to date only terrestrial species of plants or molluscs (Table 2), which requires the investigator to develop some skills in fossil identification. Brauer et al. (2014, p.49) recommend for lake or speleothem sequences that where samples known to be affected by a freshwater reservoir effect have been measured, these "must be

corrected prior to calibration by subtraction of the age offset estimated using the measured ^{14}C concentration of known age samples". In the fluvial setting, given the demonstrable variability in freshwater reservoir effect in relation to discharge, and the known large fluctuations in discharge regime over the time period of the radiocarbon technique, this is unlikely to be possible. The radiocarbon dating of aquatic species should therefore be avoided unless a 2000 year uncertainty is sufficient to answer the research question being posed.

2.4. Laboratory pretreatments

Because the concentrations of ^{14}C are so low in materials used for radiocarbon dating, the possibility of contamination with modern carbon is always present. Contamination during sample preparation can be avoided as detailed in Table 2. Removing contamination that has accumulated *in situ* requires laboratory pretreatment (Table 2) and becomes more crucial for samples near the limit of the radiocarbon technique between 30,000-50,000 ^{14}C years BP, because the amount of ^{14}C present within the sample is so low that any contamination has a much larger effect (Fig. 3). This is particularly important in many discontinuous fluvial sequences where problems with dating cannot be detected in the context of a vertical sequence.

Significant progress has been made in recent years in providing more reliable radiocarbon ages on bone and charcoal from this older time period (e.g. Higham et al., 2006; Bird et al., 1999) and these pretreatments should be used for these materials. However, fluvial sequences sometimes lack these dating materials, which are best preserved in dry, alkaline conditions (the opposite of the wet, acidic conditions often present in fluvial systems for the preservation of environmental material). There are as yet no 'stand-out' preferred pretreatments for the shell or seed material more commonly preserved in fluvial deposits, and advice should be sought from the radiocarbon laboratory with which you are working if the samples are likely to be near the limit of the technique.

3. Luminescence dating of fluvial deposits

The Optically Stimulated Luminescence (OSL) dating method is currently one of the most commonly applied to fluvial sediments because it directly dates the sand/silt grains of which such sediments are often composed. These grains enter the river system from hillslopes and then travel in suspension through the fluvial system, passing into and out of storage before final deposition (Fig. 2). This method was developed during the 1980s as an alternative to Thermoluminescence (TL). It became widely used ~15 years ago, in particular due to the development of the Single Aliquot Regenerative (SAR)

protocol (Murray and Wintle, 2000; 2003) which replaced previous additive approaches. The SAR protocol enables multiple age estimates to be measured from a single sample, generating more accurate final ages (Duller, 2008). Continuous improvements to precision and accuracy have occurred during past decades, giving the OSL method a key role in the dating of Quaternary fluvial archives. Many publications in special issues of the FLAG include an OSL-based geochronological approach (Table 1). Questions that have been answered by using this approach encompass, for example, the timing of phases of fluvial activity in relation to climate (e.g. Briant et al., 2004) or the dating of terrace bodies associated with archaeology (e.g. Cunha et al., 2012; this issue/2016).

Several relevant reviews related to the technical details of optical dating of fluvial deposits have been published (e.g. Wallinga, 2002; Rittenour, 2008), so the principles and basic procedures are here only briefly mentioned. Instead, we focus particularly on what researchers working on fluvial archives need to know to successfully apply this method to their samples. This includes sampling strategies, new protocols and statistical treatment of data required to derive reliable age estimates.

The OSL method is based on the estimation of the impact of radiation on the crystalline structure of minerals such as quartz and feldspar while they are shielded from light (e.g. Duller, 2004). The radiation (α, β, γ) comes from radionuclides which are present in the mineral and its natural environment, mainly U, Th (and their decay products) and K, with a small proportion from cosmic particles. This radiation leads to the trapping of electrons in crystalline lattice defects. The total amount of trapped electrons within a crystal is proportional to the total energy (dose) absorbed by the crystal, which naturally increases with time. As soon as the mineral is exposed to sunlight, especially during its transport, trapped electrons are released from the traps. This generates the emission of light (the luminescence signal) which can be measured following light stimulation (Huntley *et al*., 1985). The age of the sediment is then estimated by dividing the D_E (equivalent dose) by the dose rate (the rate at which the sediment is exposed to natural radiation).

It should be noted that the sensitivity of mineral grains to optical stimulation is highly variable, making some depositional settings inherently more successful than others. “Quartz grains that have undergone repeated cycles of bleaching and deposition tend to become sensitized ... and so for some samples a large fraction of quartz grains will yield a measurable OSL signal... [In contrast], samples from any environment can show poor sensitivity and highly-skewed sensitivity distributions ...[where]... 95% of the combined OSL signal comes from less than 5% of the grains” (Cunningham and Wallinga, 2012, p.17). In addition, the commonly-used SAR protocol may not be applicable for all samples.

241 Standard tests for the appropriateness of the SAR protocol include the use of a dose response test
242 (i.e. can the laboratory protocol successfully remeasure a known dose?) and the recycling ratio (i.e.
243 does the test dose successfully correct for sensitivity changes during measurement?). However,
244 recent experimental work suggests that these may be insufficient tests (Guerin et al., 2015; Timor-
245 Gabar et al., 2015). It is possible that this is due to an initial sensitivity change that is not corrected for
246 by the use of the response to a test dose.

247 *3.1. Causes of age underestimation*

248 The complexities involved in generating a luminescence signal mean that in some cases it is not
249 possible to provide a reliable age determination, either over- or under-estimating the age of the
250 sediment. Underestimation may occur when the mineral is saturated. This means that all traps have
251 been filled with electrons, thus preventing additional trapping. The measured signal will hence only
252 reflect a part of the burial duration, and the obtained age must be considered as a minimum age.
253 Saturation explains why the OSL method cannot be applied to old sediments. The age limit varies
254 between minerals, but quartz often saturates at doses of ~200-300 Gy (Table 3, Wintle and Murray,
255 2006). This makes it difficult to date sediments beyond 150 ka (except when the dose rate is quite
256 low).

257 Feldspars in contrast saturate at higher doses and may in theory be used to date Middle Pleistocene
258 sediments (Table 3). However, feldspars are affected by anomalous fading. This is the spontaneous
259 eviction of electrons from deep traps without light stimulation (Wintle, 1973) which can then lead to
260 age underestimation. Several procedures have been developed to detect and correct for anomalous
261 fading by estimating fading rates (Huntley and Lamothe, 2001). Another approach is the post-IR-IRSL
262 procedure (Thomsen et al., 2008). This procedure is based on the measurement of an elevated
263 temperature (>200°C) post-IR IRSL signal immediately after the IRSL measurement (typically
264 performed at 50 °C). The post-IR IRSL signal is characterised by a higher stability and thus yields
265 lower fading rates (Buylaert et al., 2009). However, the post-IR IRSL signal is harder to bleach than
266 the IRSL signal.

267 *3.2. Fluvial transport and incomplete bleaching: a main source of age overestimation*

268 The physical principles behind OSL suggest that the method is well suited to the study of fluvial
269 sediments, since it allows direct dating of the last transport-and-sedimentation process (Table 3).
270 However, in addition to the mineral-related issues described above, a key issue related to the dating of

fluvial sediments is the potential occurrence of incomplete bleaching. This phenomenon occurs when grains have not been exposed to sufficient daylight during transport. In this case, a part of the measured OSL signal is formed by electrons that remained trapped despite the fluvial transport (inherited component; Murray and Olley, 2002). This leads to an overestimation of the age, which is significant in the case of young sediments (less than 2 ka; Jain et al., 2004), but may also affect older sediments. For this reason, the detection and avoidance of incomplete bleaching is fundamental to obtain reliable burial ages to infer the timing of deposition.

In the case of fluvial sediments, these should be selected for sampling to maximise bleaching in the depositional setting. The degree of bleaching of the individual grains depends on two main parameters (Stokes et al., 2001): transport length, and the transport conditions. Sufficient transport is necessary to ensure complete bleaching of the signal. Studies focusing on transport length showed that the inherited signal was significantly reduced after a transport of several tens or hundreds of km (Murray and Olley, 2002). The second parameter refers to the way the grains are transported and includes, amongst others, the water turbidity and the channel depth. Grains that have been transported in a deep water column (leading to strong attenuation of the solar spectrum) and/or in turbid water may therefore be incompletely bleached (e.g. Ditlefsen, 1992). Settings in which samples are more or less likely to be completely bleached are represented in Figure 2. However, the expertise of the researcher must be employed at the site to truly maximise the likelihood of sampling completely bleached material, since the presence of turbid water or a deep water column will usually leave a sedimentary signature.

3.3. The importance of the sampling strategy

Following from this, the sampling strategy should aim to collect the potentially best bleached grains, keeping in mind that the OSL method is mainly applied to sand- (100-250 µm) or silt- (4-11 µm) sized grains. This makes it necessary to perform fine sedimentological investigations to interpret the depositional locations (i.e. channel/palaeochannels, point bar, crevasse splay, floodplain deposits). Most sediments analysed to date have been collected in channels or point bars (Figs. 2&4), as these are more clearly associated with significant transport of the grains. OSL dating of floodplain deposits is less common, but possible especially in the case of sandy facies (Keen-Zebert et al., 2013). Considering the sedimentation process is also very important, as the exposure to sunlight will be different in a flood dominated river (typical of Mediterranean or semi-arid areas) or a less ephemeral river. In the latter, presence of a more regular water flow will allow grains to be more completely

bleached, while in the former case mass transport associated with floods may prevent complete zeroing (Bartz et al., 2015).

In common with all depositional locations, the sampling should ideally be performed in thick (>30 cm both above and below the sample) homogeneous layers, to ensure that the dose rate estimation is as simple as possible (Fig. 4a). This is particularly important if the field scientist does not have access to a field gamma spectrometer which can capture the dose rate from this full radius of gamma radiation (Fig. 4b). In the common case of a thinner bed surrounded by inhomogenous sediments, detailed attention should be paid to the 'micro-stratigraphy' and small samples for laboratory dose rate measurement taken from all sediment types within a 30 cm radius of the sample. These can have sigificantly different dose rates (clays are often higher, gravels lower) and this can be adjusted for using the methods published by Aitken (1985) if such samples are taken. It is worth being aware, however, that the greater complexity of dose rates and lower likelihood of complete bleaching may make the results from such samples hard to interpret.

The choice of the mineral to be studied as a dosimeter is also crucial, if a choice is possible. Both theoretical work and comparative analyses by Wallinga et al. (2001) showed for Upper Pleistocene to Holocene sediments that quartz was a preferred dosimeter. The quartz grains are more rapidly bleached than feldspars (a few seconds vs a few tens of seconds, Huntley et al., 1985), and not affected by anomalous fading. For older deposits, trade offs must be made, and feldspars may be selected to allow dating of older deposits, with anomalous fading effects taken into account and corrected for as well as possible.

This sedimentological approach is fundamental in selecting the grains with the best properties for dating. However, it may in some cases not be sufficient to avoid heterogeneous bleaching. There are measurement protocols that seek to avoid partial bleaching by measuring or reporting only the well-bleached component within a sample (e.g. 'early background subtraction', Cunningham and Wallinga, 2010, or combined IR and OSL stimulation, Jain et al., 2005). However, none of these methods have become mainstream approaches as yet. It is also worth noting that field investigations and sampling may benefit from the use of recently developed portable readers (Sanderson and Murphy, 2010). These make it possible to broadly estimate luminescence intensities and, when combined with *insitu* gamma spectrometry, the depositional age. Whilst the precision is too low for this to replace laboratory measurements, it may be a useful tool in the case of complex depositional patterns, to detect

potentially problematic samples and guide sampling strategies (Stone et al., 2015). It has yet to be tested on fluvial sediments, or at the lower luminescence intensities typical of temperate-zone samples.

3.4. Detection of incomplete bleaching during OSL measurements and statistical treatments to address this issue

Incomplete bleaching can be detected while performing luminescence measurements in the laboratory. Large-scale assessments can be made firstly by measuring both quartz and feldspars for a given sample. As the dosimeters have different bleaching rates, obtaining comparable ages provides evidence for complete zeroing of the sediments prior to burial (Colarossi et al., 2015). The testing of modern analogues (recent sediments transported under conditions similar to those under study) may also be useful (e.g. Geach et al., 2015), provided such sediments are available.

It is possible to statistically separate different parts of the luminescence signal to isolate the 'fast' component, which is most easily bleached (e.g. Singarayer and Bailey, 2004). The most common way of detecting incomplete bleaching in the laboratory, however, is through investigation of the distribution of multiple age estimates from a sample. The SAR protocol is based on the measurement of multiple equivalent doses (from aliquots or single grains) for a given sample. The number of aliquots used varies, but Rodnight (2008) proposed 50 aliquots as a minimum based on analysis of a poorly bleached fluvial sample. In some case higher values are required or lower may be sufficient (Galbraith and Roberts, 2012). It is important that these measurements are performed on small aliquots or single grains to avoid averaging of the signal across the aliquot.

The initial assumption is that a fully bleached sample will yield consistent D_E values (excluding analytical uncertainty). Therefore, the presence of scattering in the D_E distribution is taken as an indication that some aliquots have been incompletely bleached. Whilst this is commonly represented as a histogram or probability density function, recently many workers have started to use radial plots which allow the inclusion of information on the precision of each D_E (e.g. Galbraith, 2010; Fig. 5). Use of appropriate statistical methods for plotting and choosing an average D_E has been made simpler for the non-specialist by the recent development of the R package for Luminescence dating (Kreutzer et al., 2012). The overdispersion parameter, defined as the remaining dispersion after having considered the uncertainty sources associated with the measurement, is seen as an indicator of the likely

presence of partial bleaching (Colarossi et al., 2015). However, it is difficult to propose a single threshold value for this since other parameters also influence overdispersion (Thomsen et al., 2012). Following investigation of the shape of the distribution, the D_E value used for the final age determination is derived from several 'age models' (Lauer et al., 2010), all available in the R package for Luminescence (Fuchs et al., 2015). The most commonly used are the Common Age and Central Age Models (combining the calculation of overdispersion with that of the weighted mean), which are appropriate when the overdispersion is zero or low, respectively (no significant evidence for partial bleaching). The Minimum Age Model (Galbraith and Laslett, 1993) is used for samples with higher overdispersion values to identify the most well bleached aliquots and bases the age estimate on these. Finally the Finite Mixture Model (Galbraith and Green, 1990) can be applied to single grains only (Galbraith and Robert, 2012) and allows the detection of discrete populations. In all these cases, however, the choice of the age model to be used is often subjective, since there is no set threshold value of overdispersion to use for choosing between different age models. Bayesian methods have been used for a number of years by the radiocarbon community and are useful in robustly identifying outliers and thereby increasing precision. Such approaches have recently been tested on OSL samples (e.g. Cunningham and Wallinga, 2012; Guerin et al., 2015). Cunningham and Wallinga applied a combination of bootstrap likelihoods and Bayesian methods to young (<1 ka), partially bleached samples from a vertical floodplain sequence in the Netherlands. The bootstrap likelihoods were used to provide a probability density function for each sample that was statistically appropriate for Bayesian analysis. This approach was useful in this setting, but can only be applied where there is sufficient sample density for the stratigraphical relationships to be known and the age distributions to overlap.

The need for such complex statistical treatment of the results may be considered a drawback of the luminescence dating method, since the obtained age is dependent on the model used. However, when explained fully and justified in relation to luminescence characteristics, this approach leads to greater confidence in the robustness of the results. The selection of the "best" model then derives from a rigorous analysis of all the available data, including not only the measurement values, but also the field and sedimentological evidence (which can be useful for example to assess the bleaching potential of the sediments). Furthermore, recent developments in the use of Bayesian statistics hold out a hope that a single approach to determining equivalent dose may soon be possible where stratigraphical relationships are clear.

3.5. A key issue for the future: extending OSL dating to the Middle Pleistocene

Whilst fluvial sediments of Middle Pleistocene age have been dated, especially using IRSL on feldspars, extending the age range to older sediments remains a major issue (Table 3). This is also of significant importance for the FLAG community as it will allow a longer-term reconstruction of valley evolution during the Pleistocene. Several protocols have been developed to date older sediments, including the pIR-IRSL method discussed above.

For quartz, a new approach is the measurement of the Thermally Transferred OSL signals (TT-OSL; Wang et al., 2006). These signals are observed after stimulation and heating of the quartz grains and result from a complex charge transfer associated with the heating. As they saturate at much higher doses than the OSL signal, they might be used for dating older sediments (Table 3). Arnold et al. (2015) compared single-grain TT-OSL and pIR-IRSL at the Atapuerca hominin site where independent age control is available. When they used measurement temperatures of 225 °C, they found good agreement for both methods from ~240–930 ka, though pIR-IRSL measurements at 290 °C gave overestimates. Arnold et al. (2015) argue therefore that multiple methods should be used in extended range dating, since each is more reliable in different settings. This view seems also relevant for the new developments in Luminescence dating, such as the Infra-Red Radio-Fluorescence (IR-RF) or the Violet Simulated Luminescence, for which further investigations are required prior to validate their suitability for dating ancient fluvial archives. It is worth noting that these approaches do not address uncertainties in estimating dose rates, which remain significant also at older ages.

4. Electron Spin Resonance (ESR) dating in fluvial environments

ESR is a radiation exposure (or palaeodosimetric) dating method based on the evaluation of the natural radiation dose absorbed by materials over geological times. The first application of ESR as a geochronologic tool was published by Ikeya (1975) on stalagmites from Japanese caves. Since then, the method has been used on a wide range of materials including phosphates, carbonates, and silicates (see review in Ikeya, 1993). The most popular applications in fluvial context are undoubtedly on fossil teeth and optically bleached quartz grains extracted from sediment, either for targeted dating of a given site/section (e.g. Falguères et al., 2006; Santonja et al., 2014) or for the establishment of a comprehensive chronological framework for terrace staircases (e.g. Voinchet et al., 2004; Antoine et al., 2007; Cordier et al., 2012). As with Luminescence dating, ESR dating is based on the quantification of charge trapped in the crystalline lattice of a material under the effect of natural

radioactivity. These trapped charges give rise to an ESR signal whose intensity is proportional to the radiation dose absorbed by the sample over time. The ESR age equation is similar to that used in luminescence dating and the standard analytical procedure consists in determining the two main parameters: the equivalent dose (D_E) and the dose rate. D_E is obtained using ESR spectroscopy, by artificially aging the samples at increasing doses in order to describe the behaviour of the studied signal. The dose rate is usually assessed by a combination of *in situ* and laboratory measurement using a wide range of different analytical techniques and corrected for the density of the material, its geometry and water content (see Grün, 1989 and Duval, 2016).

4.1. ESR dating of fossil teeth: on the importance of modelling uranium incorporation into dental tissues

ESR dating of fossil teeth has been first proposed in the mid-1980s as an alternative to fossil bones (see an overview by Duval, 2015 and references therein). The main difficulty of this application lies in the complexity of the system that has to be considered for the dose rate evaluation. A tooth is made from different dental tissues (dentine, enamel and, sometimes, cement). All have different characteristics in terms of composition and thickness that contribute to the irradiation of the enamel layer. Additionally, dental tissues are known to behave as open systems for U-series elements. In other words, teeth frequently experience delayed U-uptake or U-leaching processes. As a consequence, it is crucial to model the kinetics of the incorporation of U into each dental tissue in order to obtain an accurate estimation of the dose rate. The most common, and reliable, method is using the U-series data collected for each dental tissue in combination with the ESR dose evaluation (i.e., the so-called combined U-series/ESR dating approach; see Grün et al., 1988 and Grün 2009). Further detail is found in a recent review by Duval (2015) and Table 4.

4.2. ESR dating of sedimentary quartz grains: the choice of signal to measure

Similar to OSL, ESR dating of sedimentary quartz is based on the study of light-sensitive signals whose intensity is reset (bleached) under sunlight exposure during sediment transportation. Once the sediment is buried, and thus sheltered from sunlight, paramagnetic centres are created and the ESR signal intensity increases as a result of the interaction of natural radioactivity with the quartz sample. Quartz has several paramagnetic centres associated with crystal defects (for a detailed review, see Ikeya, 1993; Preusser et al., 2009), but the most widely used since the first dating application by Yokoyama et al. (1985) are undoubtedly the Titanium (Ti) and the Aluminum (Al) centres. Because Al

452 is the major trace element found in quartz (Preusser et al., 2009), the ESR signal associated with the
453 Al centre can be observed in any sample. It also usually presents high intensities (Fig. 6a) and signal-
454 to-noise ratio values, ensuring high precision measurements (Duval, 2012). However, the Al signal
455 shows relatively slow bleaching kinetics (the signal requires several hundred hours of UV laboratory
456 irradiation to reach a minimum value, see Fig. 6b), and it cannot be fully reset under sunlight exposure
457 as there is a residual ESR intensity that cannot be bleached (Fig. 6b; Toyoda et al, 2000). This
458 residual level should be assessed (usually via bleaching experiments using sunlight simulators) in
459 order to avoid dose overestimations. In contrast, the Ti centres (Ti-Li and Ti-H mostly in quartz
460 samples) show much faster bleaching kinetics and no residual (i.e. unbleachable) ESR intensity.
461 However, measurements are significantly longer and less precise than those of the Al centre given the
462 very low ESR intensities that are usually measured (Fig. 6a, Duval and Guilarte, 2015). Further detail
463 about ESR dating of optically bleached quartz grains may be found in the recent reviews by Toyoda
464 (2015) and Tissoux (2015), while basic information is also given in Table 4.

465 *4.3. Fluvial environment and ESR dating: main specificities*

466 Depending on the material dated, there may be different impacts from the fluvial environment on the
467 ESR dating results. Unlike in quartz, the ESR signal measured in tooth enamel is not light sensitive
468 and thus cannot be reset during transportation. However, transport and depositional conditions can
469 indirectly impact the ESR results, in particular regarding the preservation state of the sample, as they
470 may fragment and weaken dental tissues, thus favouring post-depositional processes and in particular
471 U-uptake or leaching. Additionally, a review by Grün (2009) showed that the U-uptake kinetics into
472 dental tissue is significantly different depending on the sedimentary environment: teeth found in cave
473 sites most frequently document earlier U-uptake compared with those found in open air sites, which
474 also show more frequent occurrences of U-leaching. This is most likely due to differences in the
475 sedimentological context. Cave sites, as closed environments, usually offer more stable geochemical
476 conditions over time. In contrast, open air sites are frequently found as the result of erosion processes
477 that may induce modifications of the hydrological environment and cause recent mobilisation of
478 radioelements impacting the original isotopic signature of the teeth.

479 Fluvial transport has a direct impact on the ESR signals measured in quartz as it is known to induce
480 resetting by either exposure to natural sunlight (Toyoda et al., 2000) or mechanical effects (Grün and
481 Liu, 2011). Similarly to OSL, the degree of bleaching of the ESR signals depends on the length and

conditions of transport (see section 3.2.). In a recent study, Voinchet et al. (2015) studied the impact of a series of parameters such as the grain size, transport mode and water turbidity to evaluate the most suitable conditions for optimum bleaching. Based on their results, higher bleaching levels were achieved for 100-200 µm grains in comparison with other fractions and for fluvial transport under clear water conditions (see overview in Fig. 2).

4.4. Sampling precautions

When dating sedimentary quartz, sampling precautions are very similar to those for Luminescence dating (section 3.3), i.e. the choice of a suitable sedimentary setting and suitably thick beds for simplicity of dose-rate estimation (Fig. 4). Although ESR signals bleach much slower than OSL ones, it is nevertheless important to minimise the exposure of the raw sediment to the sunlight during sampling, as in luminescence dating. According to the results shown by Voinchet et al (2015), sediment showing a non-negligible fraction of medium sands (mostly 100-200 µm) and transported and deposited in a clear-water fluvial environment should be targeted for sampling, as they potentially offer the most suitable bleaching conditions. In addition, *in situ* measurements of natural radioactivity should be undertaken (especially if the immediate surrounding sedimentary environment is not homogeneous, see Fig. 4b), in order to obtain an accurate estimation of the gamma dose rate. Additional small bags of sediment are also usually collected at the ESR sampling spot for future laboratory analysis, e.g. for water content evaluation and analysis of radioelement concentration. When dating teeth, samples have usually already been collected during the archaeo-palaeontological excavation and are thus chosen from collections. It is important to make sure that exact original (geographical and stratigraphical) location of the selected tooth is well-known and the corresponding layer/outcrop/site is still accessible to enable complementary fieldwork sampling and dose rate measurements. Ideally, in the case of fossil teeth it is recommended to ask the archaeologists and/or palaeontologists to collect the sediment attached to the tooth during the excavation. This is essential for a correct evaluation of the beta, and sometimes gamma, dose rate component(s). The apparent preservation state of the tooth matters as well, as previous studies have shown a strong correlation between macroscopic cracks in dental tissues and preferential migration of U-series elements (Duval et al., 2011).

4.5. Current challenges in ESR dating

4.5.1. ESR dating of fossil tooth enamel: improving resolution and removing unstable components of the ESR signal

In comparison with quartz, ESR dose reconstruction of fossil tooth enamel is more straightforward. The composition of the ESR signal and its dose response has been extensively studied in recent decades. The modern development of ESR analyses of enamel fragments now enables the differentiation of the relative contribution of non-oriented CO_2^- radicals (NOCORs) vs. the oriented ones (CORs) (e.g. Grün et al., 2008). Additionally, Joannes-Boyau and Grün (2011) showed that laboratory gamma irradiation produces additional unstable NOCORs in comparison with natural irradiation, which may lead to dose underestimation (~30%) if this contribution is not removed. The authors acknowledge, however, that this value should not be considered as universal and extrapolated to any samples, as it may depend on many parameters (e.g., age, type, species). In contrast, more recent investigations indicate that this preferential creation of an unstable component may not be systematic, being rather sample dependant (Duval and Grün, unpublished data). Consequently, from these results it seems that each sample should be independently assessed. However, as an additional complication, it should be mentioned here that most of the dating studies are performed on enamel powder. One of the major current challenges would thus be to develop an analytical procedure that enables an easy identification of these unstable NOCORs using enamel powder. In that regard, using the microwave saturation characteristics of the different groups of CO_2^- (Scherbina and Brik, 2000) may be an avenue worth exploring in the future.

High resolution LA-ICP-MS U-series analyses has recently demonstrated the spatial heterogeneity of the distribution of U-series elements in dental tissues (Duval et al., 2011). This analytical tool has rapidly become essential for studying U-mobility and may be particularly useful to identify domains in the teeth that are suitable for ESR dating. However, the use of this technique raises new issues. There is a difference in resolution when comparing ESR and the ICP-MS methods. Currently, *in situ* laser ablation ICP-MS U-series analysis can be performed with a resolution of a few tens of µm. In contrast, the spatial variation of the ESR signal intensity in tooth enamel has rarely been studied, and ESR bulk analyses are usually performed on several hundreds of mg of enamel powder. This difference in resolution may become a non-negligible source of uncertainty in ESR dating, especially for old samples for which the dose rate associated with dental tissues is the major factor in the total dose rate calculation. Future challenges will thus consist of developing new approaches to reduce the amount of sample required for ESR analyses and obtain spatially resolved data. This is now possible through the

use of high sensitivity X-band resonators and with the development of a specific analytical procedure for quantitative measurements in Q-band spectroscopy based on only a few mg of enamel (Guilarte et al., 2016). Additionnally, although it is for the moment extremely complicated to integrate spatially resolved ESR and U-series data for age calculations, the recent development of DosiVox (software for dosimetry simulations) opens new possibilities for modelling dose rates from complex geometries and heterogeneous spatial distributions of radioelements (Martin et al., 2015).

4.5.2. Avoiding and minimizing the effect of scatter and incomplete bleaching in ESR dating of sedimentary quartz

One of the main difficulties in ESR dating of quartz is to achieve repeatable measurements ensuring reproducible D_E results. This reproducibility is lower than that obtained with tooth enamel, not only because measurements close to liquid N_2 temperature require a very stable experimental setup, but also because of the heterogeneity of the quartz samples and the strong angular dependence of the signal within the cavity. Extensive work has been performed recently to optimise the conditions of measurements for both the Al and Ti centres (e.g. Duval and Guilarte, 2012, 2015; Duval, 2012).

In parallel to this work, another major challenge is in reducing the uncertainty on the final D_E value. As noted by Toyoda (2015), some approaches developed in OSL dating are definitely worth exploring in ESR dating. Perhaps the most obvious is the use of the regenerative dose protocol instead of the additive dose protocol that is routinely used in ESR. This protocol would not only provide more precise D_E results but also significantly shorten the analytical time (i.e. fewer aliquots to be measured and lower irradiation dose values). However, several previous attempts employing optical bleaching resetting have shown somewhat contrasting results regarding the presence of sensitivity changes (Tissoux et al., 2007; Beerten and Stesmans, 2006). Other approaches are less obviously fruitful. For example, although single grain dating using Q-band ESR spectroscopy has been tested to identify partial bleaching among a grain population, it is currently too complicated to be applied routinely (Beerten and Stesman, 2006).

The main challenge, however, is in minimising the uncertainty regarding possible incomplete bleaching of the signal during sediment transportation. Most dating studies use the Al centre even though laboratory bleaching experiments indicate that several hundreds of hours of exposure to UV are required for the ESR signal to decay to a plateau (e.g. Toyoda et al., 2000; see also Fig. 6b). These values would correspond to several tens of days of sunlight, which understandably leads many

authors to question the possibility of the Al centre actually reaching its residual ESR intensity during transportation. However, Voinchet et al. (2007) demonstrated that the signal was fully reset (to its residual level) after only 1 km of transportation in the Creuse river, France. Additionally, at the Vallparadís site (Spain), Al-ESR ages were found to be in good agreement with the US-ESR ages on fossil teeth and data from magneto- and bio-stratigraphy (Duval et al., 2015). These two examples demonstrate that any definitive conclusion derived from laboratory bleaching experiments should be considered with caution. It is possible that other processes, not yet understood, are involved in the bleaching of the signal in natural conditions.

As a consequence of the uncertainty that may arise from the bleaching of the Al centre, ESR age results based on this centre should be considered as maximum possible ages: the true age of the deposits being either similar or younger. To constrain this uncertainty, a few strategies are available. The use of modern analogue samples collected from nearby river banks may provide some useful information regarding resetting of the signal. This approach is, however, based on the assumption that transportation and bleaching conditions are similar to those in the past, which is not always plausible. Another approach is to use independent age control to verify the age results (see the example of Vallparadís, Duval et al., 2015). However, the best option is undoubtedly the Multiple Centres (MC) approach proposed by Toyoda et al (2000). The authors proposed the systematic measurement of both the Ti-Li and Al centres in quartz samples in order to check whether they would provide consistent results (Table 5). If the Al centre yields an age estimate older than that of the Ti centre, this is interpreted as incomplete bleaching of the Al signal. In this case, the Ti-Li age should be considered a closer estimate to the burial age of the deposits. Although ESR measurements following the MC approach are highly time consuming, it has provided promising results (see Rink et al., 2007; Duval et al., 2015). The use of this MC may soon become a standard requirement in ESR dating of optically bleached quartz grains.

Lastly, another Ti centre, Ti-H, presents great potential worth investigating for dating purposes. It is known to bleach much faster and to be more radiosensitive than the Ti-Li (see Fig. 6b; Duval and Guilarte, 2015), which would make it a good candidate for dating deposits younger than 200 ka. It is, however, unclear for the moment whether it provides reliable dose estimations. Indeed, the weakness of the signal intensity makes it very complicated to measure in all samples, resulting in low measurement precision (Table 5; Duval and Guilarte, 2015).

5. ^{230}Th/U-dating of fluvial deposits

The ^{230}Th/U-dating method is based on the radioactive decay in the natural decay chain of ^{238}U and was developed in the 1960s (Broecker, 1963; Kaufman and Broecker, 1965). Since then, the precision and accuracy of the method has progressively increased, primarily due to major technical advances. Whereas alpha spectrometry was widely used until the 1990s (Goldstein and Stirling, 2003), the use of thermal ionisation mass spectrometry (TIMS) (Edwards et al., 1987) represented a major advance at the end of the 1980s. This reduced the time required for an analysis from a week to several hours, decreased sample size from 10-100 g to 0.1-1 g and, most importantly, improved precision from percent to permil levels and extending the dating range from 350 to 600 ka (Goldstein and Stirling, 2003). In the last two decades, the application of multi-collector inductively coupled plasma mass spectrometry (MC-ICPMS) has led to further substantial improvements (Goldstein and Stirling, 2003; Scholz and Hoffmann, 2008). The considerably higher ionisation and transfer efficiency for U and Th isotopes of the MC-ICPMS technique leads to higher count rates, in turn resulting in more precise and accurate ^{230}Th/U-ages. Furthermore, measurement times (~10-20 minutes) and sample sizes are again substantially lower than for TIMS. In addition to the technical advances, the half-lives of both ^{230}Th and ^{234}U have been re-determined (Cheng et al., 2000, 2013), also leading to more precise ^{230}Th/U-ages. During the last decade, procedures for laser-ablation (LA) MC-ICPMS ^{230}Th/U-dating of carbonates have been developed (e.g. Eggins et al., 2005; Mertz-Kraus et al., 2010). This technique has very large potential since it offers *in situ* dating at extremely high spatial resolution (in the range of 10-100 µm), requires no sample preparation and is extremely fast and, thus, enables very high sample throughput. In return, the analytical precision is much lower than for conventional ^{230}Th/U-ages (a few percent compared to epsilon levels).

In undisturbed natural materials with an age of several million years, the activity of the parent (i.e. ^{238}U) and the daughter isotopes (i.e. ^{234}U and ^{230}Th, respectively) is in secular equilibrium. This state of equilibrium, however, can be disturbed by several natural processes, which is the basic principle of all U-series disequilibrium dating methods. In aqueous environments, the major reason for disequilibrium between U and Th is the different geochemical behaviour of the two elements. Whereas U is soluble, Th is insoluble in natural waters and, thus, mainly transported adsorbed onto particles. As a consequence, groundwater, rivers, lakes and seawater contain significant amounts of dissolved U, but essentially no Th. During formation of secondary carbonates, U is thus incorporated, whereas Th is not. Consequently, secular equilibrium is disturbed, and the initial activity of ^{230}Th is zero. If the decay

633 system remains closed after deposition (i.e. no U and Th isotopes are lost or added subsequently), the
634 activity ratios of ($^{234}U/^{238}U$) and ($^{230}Th/^{238}U$) return to the state of secular equilibrium (e.g. Bourdon et
635 al., 2003, activity ratios are indicated in parentheses in the following). The temporal evolution of the
636 activity ratios (in particular the increase of ^{230}Th due to the decay of ^{234}U and ^{238}U) allows dating of the
637 time of carbonate formation (i.e. the timing of the establishment of disequilibrium) and, thus, the age of
638 the carbonate phase. This is, however, only possible if two basic requirements are fulfilled: (i) no
639 presence of initial ^{230}Th and (ii) the system remained closed after deposition. If one of these
640 assumptions is violated, the resulting $^{230}Th/U$-age may be substantially inaccurate.

641 $^{230}Th/U$-dating can, in principle, be applied to all materials whose formation is accompanied by a
642 constrained disequilibrium between U and Th. The materials most widely dated by the $^{230}Th/U$-method
643 are fossil reef corals and speleothems (Scholz and Hoffmann, 2008; Edwards et al., 2003), which can,
644 in general, be accurately and precisely dated up to an age of 600 ka. However, with increasing
645 sensitivity of both LA and MC-ICPMS systems, increasing precision may be achieved enabling high-
646 precision *in situ* $^{230}Th/U$-dating (i.e., without prior sample preparation) at very high spatial resolution.
647 This may be particularly useful for impure carbonates found in fluvial deposits in order to analyse the
648 most pristine fractions of a dirty sample. Examples of successful dating of inclusions in fluvial deposits
649 by the $^{230}Th/U$-method (Fig. 2) include pedogenic carbonates and calcretes deposited in alluvial fans
650 and river terraces (e.g. Candy et al., 2004; Kelly et al., 2000; Ludwig and Paces, 2002; Sharp et al.,
651 2003) as well as tufa and travertine (Schulte et al., 2008; Candy and Schreve, 2007). All these
652 deposits have in common that they form subsequently to the deposition of fluvial sediments, such as
653 fans and terraces (Fig. 2). Thus, they can only provide a minimum age for the fluvial deposits with
654 which they are associated (Blisniuk et al., 2012). Carbonates that have been mobilised subsequent to
655 deposition (e.g. flood events or washed in from slopes, Fig. 2) are not expected to provide reliable
656 $^{230}Th/U$-ages because they are (i) most likely affected by post-depositional diagenesis and (ii) difficult
657 to relate to a depositional context (Fig. 2). Extensive reviews of the $^{230}Th/U$-dating methodology can be
658 found in the classic books by Ivanovich and Harmon (1992) and Bourdon et al. (2003).

659 *5.1. $^{230}Th/U$-dating of secondary carbonates in fluvial archives: main issues*

660 In general, carbonates deposited in fluvial and lacustrine environments are difficult to date by the
661 $^{230}Th/U$-method. In many cases, samples of fluvial and lacustrine deposits contain very large amounts
662 of detrital Th, which represents a violation of one of the basic requirements of the dating method.

Since Th is mainly transported adsorbed onto particles, it is generally associated with relatively fast flowing water, which has the potential to transport these particles. In particular, carbonates associated with alluvial fans thus often contain substantial amounts of detrital Th (Fig. 2). However, pedogenic carbonates may also contain high amounts of detrital Th, which is mobilised from the overlying horizons (Fig. 2). These materials are thus often referred to as impure carbonates or dirty calcites (e.g., Kaufman, 1993). Initial Th is often associated with a silicate or clay fraction. Whereas the preparation of pure carbonate samples is relatively straightforward (e.g. Yang et al., 2015), the preparation of impure carbonates may be more elaborate due to the presence of an insoluble residue. Various approaches to deal with insoluble residues have been proposed (see section 5.2.2). Initial (also often referred to as *detrital*) ^{230}Th is generally accompanied by ^{232}Th, which is the most abundant naturally occurring isotope of Th. ^{232}Th does not occur in the decay chain of ^{238}U and is, in contrast to ^{230}Th, not produced by the decay of ^{234}U and ^{238}U. Elevated content of ^{232}Th is clear evidence for the presence of initial ^{230}Th, and its concentration even provides a measure for the degree of contamination. For (^{230}Th/^{232}Th) activity ratios <20, a correction for detrital contamination is definitely required (Schwarcz, 1989). Other studies have suggested even higher thresholds for (^{230}Th/^{232}Th) necessitating a correction for detrital contamination (Richards and Dorale, 2003). Potential correction techniques that have been shown to be successful for fluvial deposits are discussed in sections 5.2.1. and 5.2.2. In addition, post-depositional open-system behaviour is not uncommon for secondary carbonates deposited in fluvial environments, which is even more complicated to detect and account for (see 5.2.3.). For marine samples, such as corals, open system behaviour can be detected by comparing the initial (^{234}U/^{238}U) activity ratio of the sample with the (^{234}U/^{238}U) activity ratio of modern seawater (e.g. Edwards et al., 2003). In terrestrial environments, this is not possible due to the highly variable (^{234}U/^{238}U) activity ratio in river, lake and groundwater. Thus, successful ^{230}Th/U-dating of fluvial carbonates has been restricted to a relatively small number of case studies, which are characterised by the high U content (^{238}U>1 µg/g) of the dated material.

5.2. Approaches developed to date secondary carbonates by ^{230}Th/U

Two general correction methods to account for detrital Th have been developed: *a priori* estimation of the (^{230}Th/^{232}Th) activity ratio of the detrital phase and isochron techniques. In rare cases, secondary carbonates associated with fluvial deposits, such as tufa and travertine, may be very clean, and a correction for initial ^{230}Th may not be necessary. For instance, Schulte et al. (2008) established a chronology for the fluvial terrace sequence from the River Aguas basin, Iberian Peninsula, by ^{230}Th/U-

694 dating of travertine. The (^{230}Th/^{232}Th) activity of some of their samples is larger than 20, and a
695 correction for initial ^{230}Th is not required. Candy and Schreve (2007) obtained ^{230}Th/U-ages on fluvial
696 and colluvial tufa deposits from southern England with sufficient precision to correlate discrete periods
697 of temperate climate with individual warm sub-stages during MIS 7. Although the U content of their
698 samples is relatively low (ca. 0.1 µg/g), the (^{230}Th/^{232}Th) activity of the majority of samples is >20.

699 *5.2.1. A priori estimation of the (^{230}Th/^{232}Th) activity ratio of the detrital phase*

700 The average ^{232}Th/^{238}U weight ratio of the upper continental crust is ~3.8 (Wedepohl, 1995). Assuming
701 secular equilibrium between ^{230}Th, ^{234}U and ^{238}U for the detrital component, the (^{230}Th/^{232}Th) activity
702 ratio of the initial Th is ~0.9 (Hellstrom, 2006). Based on the measured content of ^{232}Th, the amount of
703 initial (detrital) ^{230}Th can thus be estimated and subtracted from the measured concentration of ^{230}Th.
704 This approach is often referred to as *a priori* estimation of the detrital phase and may provide
705 reasonable ages. However, the initial (^{230}Th/^{232}Th) activity ratio is highly variable and associated with
706 large uncertainties. Usually, an uncertainty of 50% is assumed (Hellstrom, 2006). Propagation of this
707 substantial uncertainty to the corrected ^{230}Th/U-age may lead to highly elevated age uncertainties and
708 even ages with zero significance (Kaufman, 1993; Wenz et al., 2016). Despite these large
709 uncertainties, *a priori* estimation of the (^{230}Th/^{232}Th) activity ratio of the detrital phase has been
710 successfully applied to date fluvial deposits by the ^{230}Th/U-method. For instance, Adamson et al.
711 (2014) obtained a large number of ages for fluvial deposits in Montenegro by ^{230}Th/U-dating of
712 carbonate benches and calcite rinds. This study is particularly remarkable because the U content of
713 the studied samples was relatively low (<1 µg/g). However, many samples also have very low ^{232}Th,
714 resulting in (^{230}Th/^{232}Th) activity ratios >20. Ludwig and Paces (2002) determined ^{230}Th/U-ages on
715 pedogenic silica-carbonate clast rinds and matrix laminae from alluvium in Crater Flat, Nevada,
716 employing the TSD-technique, whereas Sharp et al. (2003) dated pedogenic carbonate clast-rinds
717 from gravels of glacio-fluvial terraces in the Wind River Basin, Wyoming. The success of both studies
718 is mainly based on the high U content of the samples. Blisniuk and Sharp (2003) determined the age
719 of two well-preserved fluvial terrace surfaces in central Tibet by ^{230}Th/U-dating of pedogenic carbonate
720 rinds on clasts in the terrace deposits.

721 *5.2.2. Isochron methods*

722 The second approach to account for initial or detrital ^{230}Th is the isochron methodology. For isochron
723 ^{230}Th/U-dating of impure carbonates, various procedures for sample preparation have been proposed

(e.g. total sample dissolution (TSD), leachate-leachate (L/L), leachate-residue (L/R), Bischoff and Fitzpatrick, 1991; Kaufman, 1993; Ku and Liang, 1984; Luo and Ku, 1991; Schwarcz and Latham, 1989). In addition, several statistical methods for the evaluation of the isochron data have been developed (Ludwig, 2003). In general, the isochron method is more flexible than the *a priori* approach and provides more reliable ages with smaller uncertainties (Wenz et al., 2016). However, the application of the isochron methodology is based on two assumptions: all sub-samples (i) must have the same age and (ii) should contain different amounts of the same detrital component (i.e. with the same ($^{234}U/^{238}U$) and ($^{230}Th/^{238}U$) ratios). Unfortunately, the latter assumption in particular is not fulfilled for many impure carbonate samples (Ludwig, 2003; Wenz et al., 2016), again leading to large age uncertainties and corrected ages with low significance. Isochron techniques have also been successfully applied for ^{230}Th/U-dating of fluvial deposits. For instance, a stratigraphically consistent chronology based on isochron ^{230}Th/U-ages determined on pedogenic calcretes has been reported for alluvial terrace sequences from the Sorbas Basin, south-eastern Spain (Candy et al., 2004, 2005; Kelly et al., 2000). However, Candy et al. (2005) have shown that dating of mature calcretes is much more difficult than dating of immature calcretes, as has been revealed by the isochron statistics. Nevertheless, it may also be possible to determine a reliable age for mature calcretes if a large number of sub-samples from a single horizon are dated. Other studies aiming to date fluvial deposits were not successful in accounting for initial ^{230}Th by isochron techniques. For instance, Kock et al. (2009) attempted ^{230}Th/U-dating of pedogenic carbonate crusts from fluvial gravels of the River Rhine, and compared them with internally coherent OSL ages. Most of their U-series data scattered widely on isochron diagrams suggesting multiple components of initial ^{230}Th that are not related to detrital ^{232}Th. A significant fraction of the initial ^{230}Th may originate from bacterial activity and Th transport on organic colloids. This suggests that samples in which bacteria could have contributed to carbonate precipitation should be avoided.

5.2.3. Accounting for open-system behaviour

One option for detecting open-system behaviour of ^{230}Th/U-ages of fluvial deposits is through comparison with independent ages (e.g. Blisniuk et al., 2012; see section 7). Another option is consideration of the stratigraphical context of the deposited samples, i.e. whether the determined (corrected) ^{230}Th/U-ages are in stratigraphical order within a sedimentary sequence. This approach is currently used to identify ages representing outliers, probably because the applied correction techniques were not successful or due to post-depositional open-system behaviour. This approach

has been proved to be successful for the aragonitic lacustrine sediments from Lake Lisan, the Last Glacial precursor of the Dead Sea, which have been extensively studied by ^{230}Th/U-dating (e.g., Torfstein et al., 2013). These sediments contain high amounts of U (>3 µg/g), and different approaches have been used to obtain corrected ages, including isochrons (Schramm et al., 2000), *a priori* estimates of the detrital (^{230}Th/^{232}Th) activity ratio (Schramm et al., 2000) and an iterative approach independently evaluating the composition of the detrital component for every set of coeval samples (Torfstein et al., 2013). Furthermore, several authors recently have suggested algorithms for speleothems including stratigraphical constraints in order to estimate the (^{230}Th/^{232}Th) activity ratio of the detrital component (Hellstrom, 2006; Roy-Barman and Pons-Branchu, 2016). These algorithms may also be very useful for fluvial samples deposited in a clear stratigraphical context.

6. Terrestrial cosmogenic nuclides (TCN) dating of fluvial deposits

The development of the AMS technology in the early 1980s (e.g. Klein et al., 1982), which allowed measurements of isotopic ratios as low as 10^{-15} at that time (presently 10^{-16} has been reached), represented a decisive milestone, enabling the use of TCN as a dating tool, as proposed by Davis and Schaeffer (1955). In parallel, a tremendous amount of work has taken place and aimed at understanding the physical properties and processes involved in the production of the most commonly used nuclides in the Earth sciences, i.e. ^{3}He, ^{10}Be, ^{21}Ne, ^{26}Al and ^{36}Cl (e.g. Nishiizumi et al., 1986; see reviews of Gosse and Philips, 2001; Dunai, 2010). A particular emphasis was on the determination and refinement of their respective production rates according to the different production pathways, mostly involving fast neutron- (spallation) and muon-induced reactions (Gosse and Philips, 2001). This is well exemplified by the strongly debated determination of both the production rate of ^{10}Be in quartz and the half-life of this radionuclide (Gosse and Philips, 2001; Dunai, 2010). Moreover, the use of these nuclides as geochronometers required integrating the variability of production rates in space and time, hence the build-up of scaling factors (Dunai, 2010).

Depending on the aim of the study and/or the fluvial or lacustrine environment where it takes place, numerical ages based on concentration measurements of cosmogenic nuclides can be undertaken either via surface exposure dating or burial dating (Fig. 2). Both dating approaches are presented in this section. Note that the material that has to be dated undergoes pre-exposure to cosmic rays during (i) bedrock exhumation, (ii) temporary storage on hillslopes and (iii) transport and/or temporary storage in the fluvial system (Fig. 2). This accumulation of cosmogenic nuclides inventories prior to the

785 depositional event is known as inheritance (Anderson et al., 1996). Whereas surface exposure dating
786 of depositional landforms is highly sensitive to this process (see 6.1), this inherited component allows
787 the dating of a burial event (see 6.2). In fluvial settings, surface exposure dating first provided
788 numerical ages for alluvial fans (Siame et al., 1997; Van der Woerd et al., 1998) and river terraces,
789 both bedrock strath terraces (Burbank et al., 1996; Leland et al., 1998) and alluvium-mantled terraces
790 (Anderson et al., 1996, Repka et al., 1997). In lacustrine environments, surface exposure dating of
791 palaeo-shorelines provides information about former lake-level highstands (Rades et al., 2013). Burial
792 dating can be applied to in cave-deposited alluvium (Granger et al., 1997) or deeply buried fluvial or
793 lacustrine sediments (Kong et al., 2009).

794 *6.1. Surface exposure dating*

795 The calculation of exposure ages requires both high-precision AMS measurements of nuclide
796 concentrations and the determination of the site-specific nuclide production rate. The latter must
797 integrate the use of specific scaling factors and the potential topographic or self shielding of cosmic
798 rays at the sampling location (Dunai, 2010). As fluvial sediments or related landforms very often
799 contain quartz-bearing material, surface exposure ages are usually determined via concentration
800 measurements of ^{10}Be (Fig. 7a, Dunai, 2010), sometimes used alongside ^{26}Al (e.g. Repka et al., 1997;
801 Rixhon et al., 2011). However, alternative nuclide species are produced in other minerals, such as ^{3}He
802 in olivine and pyroxene or ^{36}Cl in calcite (see Gosse & Phillips, 2001; Dunai, 2010), thereby allowing
803 other lithologies to be dated (e.g. Baynes et al., 2015). The dateable range in surface exposure dating
804 of fluvial environments varies strongly according to the setting and the employed nuclide(s) (Fig. 1).
805 The lower age range very much depends on the detection limit of the AMS, hence the production
806 rates, but late Holocene exposure ages of bedrock strath surfaces were obtained (Leland et al., 1998,
807 see 6.1.2.). On the other hand, surface exposure dating with ^{10}Be, because of its long half-life (i.e.
808 ~1.36 Ma), permits pre-Quaternary applications under specific conditions without saturation being
809 reached (Dunai, 2010).

810 In many instances, surface exposure ages of fluvial depositional surfaces, especially alluvial fans,
811 were formerly based on concentration data obtained from individual clasts or boulders lying on these
812 (Fig. 7a, b; e.g. Siame et al., 1997; Van der Woerd et al., 1998). However, Schmidt et al. (2011)
813 emphasized the need of caution when inferring exposure ages from such TCN concentration data;
814 diverse geomorphological processes acting on a surface might indeed represent a considerable

source of uncertainty. These encompass inheritance (Fig. 2), post-depositional weathering, erosion or covering by sediments and even by snow (e.g. Anderson et al., 1996; Rixhon et al., 2011). Whereas inheritance might lead to an overestimate of the true exposure age, all other processes tend to reduce the cosmogenic inventory near the dated surfaces and thereby result in age underestimations. An unequal distribution and/or intensity of these stochastic processes across the surface might result in a significant spread in apparent exposure ages (Owen et al., 2014). For this reason thorough field observations and descriptions are an absolute prerequisite for surface exposure sampling (see field template in Dunai, 2010).

6.1.1. Depth profile dating of depositional surfaces (alluvial fans, alluvium-mantled terraces)

The depth profile sampling technique may overcome some of the uncertainties related to these geomorphological processes (Anderson et al., 1996). It allows simultaneous computation of exposure time (i.e. the abandonment time of the landform), the post-depositional denudation rate of the landform and inheritance (Braucher et al., 2009; Hidy et al., 2010). This approach consists of sampling the fluvial sediments at regular depth intervals (Fig. 7c), taking advantage of the spallation-dominated production at or near the surface and the muon-dominated production at greater depth (Braucher et al., 2009). Given the physical properties of these particles, an exponential decrease of TCN concentrations along the depth profile is expected and can be modelled by Monte Carlo simulations (Fig. 7d, see the user-friendly simulator of Hidy et al., 2010). However, because this method is very sensitive to any post-depositional reworking processes (e.g. cryo- or bioturbation…), one should avoid sites where such processes have occurred.

The depth profile technique is particularly useful for dating alluvial fans and fill terraces (Fig. 7d, e.g. Repka et al., 1997; Le Dortz et al., 2011; Rixhon et al., 2011). In contrast to the pioneering studies on alluvial fans (e.g. Siame et al., 1997), almost all recent works systematically combined surface concentration data with depth profile data to better constrain the inheritance and the post-depositional evolution of the landform (e.g. Le Dortz et al., 2011; Schmidt et al., 2011; Owen et al., 2014). Where the petrographic composition of fan - or terrace - sediments is favourable, it is advisable to perform an internal control by comparing concentrations of different nuclides. For instance, quartz-bearing and calcite-bearing materials enable ^{10}Be and ^{36}Cl concentration measurements, respectively (Le Dortz et al., 2011). As lateral or vertical offsets disrupting fan surfaces represent an excellent geomorphological marker for crustal deformation, surface exposure ages allow quantifying average

slip rates along main fault lines for the Middle/Late Pleistocene and/or the Holocene (e.g. Siame et al., 1997; Le Dortz et al., 2011). Also, surface exposure dating of fan surfaces may likewise provide valuable information about climatic forcing on fan formation (e.g. Owen et al., 2014). Depth profile concentration data of terrace sediments are commonly used to quantify incision rates by sampling vertically-spaced levels within terrace sequences (e.g. Repka et al., 1997). Alternatively, diachronic abandonment times of geometrically-correlated terraces along a hydrological network allow inference of long-term propagation rates of a specific incision wave from the main trunk into its (sub-)tributaries (Rixhon et al., 2011).

6.1.2. Surface exposure dating of strath terraces

An alternative application of the surface exposure method consists of dating bedrock surfaces of strath terraces (Fig. 2). This term is used here to describe laterally-carved benches in steep valley flanks, especially in actively uplifting orogens (e.g. Himalayas), and are often characterized by smooth polished surfaces or sculpted erosional features (Fig. 7e, Burbank et al., 1996; Leland et al., 1998). Inheritance usually does not represent a major issue for strath terraces since they are erosional landforms. Provided that the bedrock surface is still pristine, one can assume insignificant weathering or erosion after strath abandonment. If the strath was not covered by temporary alluvium or landslide deposits subsequent to terrace abandonment (see Leland et al., 1998), the calculation of the exposure time is straightforward (Fig. 7f, g). To check the representativeness of bedrock samples and to take concentration variability into account, we recommend the nested sampling strategy of Reusser et al. (2006). The thin alluvial cover can also be sampled if it is present (e.g. Reusser et al., 2006). Surface exposure dating of strath terraces in diverse gorge settings highlighted, for instance, (i) differential rock uplift related to major thrust activity in active orogens (Burbank et al., 1996; Leland et al., 1998), (ii) regional, climatically-driven incision of rivers along a passive margin (Fig. 7f, g, Reusser et al., 2006) or (iii) the impact of extreme flood events for canyon formation related to significant knickpoint retreat (Baynes et al., 2015).

6.2 Burial dating

In contrast to surface exposure dating, which relies on continuous accumulation of TCN, burial dating is based on the differential decay of at least two nuclides, where at least one of them is a radionuclide – for full details, see Granger and Muzikar (2001) and Granger (2014). The nuclide pair $^{26}Al/^{10}Be$ is frequently employed because they are both produced in quartz and their production ratio is

875 fundamentally independent from latitude and altitude and varies only slightly with depth (Dunai, 2010;
876 Granger, 2014). In the case of the pair ^{26}Al and ^{10}Be, burial dating is based on a two step
877 exposure/shielding episode of any quartz-bearing material. First, the latter accumulates nuclide
878 inventories during exhumation of bedrock and transport/storage on hillslopes and in the drainage
879 network (Fig. 2), i.e. the inherited component. Whilst the amount of both nuclides in any given clast or
880 grain is impossible to predict due to stochastic individual exposure history, ^{10}Be and ^{26}Al
881 concentrations are related as they are produced in the same material over the same time period,
882 resulting in a ^{26}Al/^{10}Be surface concentration ratio of ~6.75:1 (Dunai, 2010; Granger, 2014). Second,
883 the quartz-bearing material is rapidly buried (see section 6.2.1.), implying a cessation of production
884 (Fig. 2). Exploiting the differential radioactive decays of both nuclides, the preburial ratio decreases
885 with increasing burial duration according to the corresponding half-lives of each nuclide (Dunai, 2010).
886 The time range of application of burial dating extends into the Pliocene (~up to 5 Ma; Fig. 1) but the
887 current analytical precision of ^{26}Al measurements in AMS implies uncertainties of (at least) ~60 to 100
888 ka (Dunai, 2010; Granger, 2014).

889 *6.2.1. Complete and fast burial: dating of in cave-deposited alluvium*

890 Fast and complete burial of sediments requires two basic assumptions (Granger and Muzikar, 2001).
891 First, the time span over which incomplete shielding occurs is much shorter than the subsequent burial
892 duration. Second, shielded sediments are buried sufficiently deeply, i.e. in practice ≥30 m, implying an
893 insignificant production through muons at depth. Given that these prerequisites are frequently met for
894 in-cave deposited alluvium (Fig. 2), the sampling of these sediments is one of the most straightforward
895 applications of burial dating (Dunai, 2010). River sediments washed into abandoned phreatic tubes in
896 limestone valley walls characterize the last time the passage was at the local water table (Fig. 8a,
897 Anthony and Granger, 2007). Alluvium-filled multi-level cave systems thus mimic alluvium-mantled
898 terrace staircases and, as such, also record the regional incision history of river systems (Fig. 8b,
899 Anthony and Granger, 2007). The selection of suitable sampling sites should ensure that abandoned
900 and alluvium-filled phreatic tubes were not contaminated by any reworked material from an older (or
901 younger) depositional episode (Dunai, 2010). The solution of the complete and fast burial dating
902 equations is graphically expressed on the so-called erosion-burial diagram, where the ^{26}Al/^{10}Be ratio is
903 plotted against ^{10}Be concentrations (Fig. 8c). This approach has provided valuable new insights into
904 long-term incision rates in diverse tectonically-active (Fig. 8b, e.g. Stock et al., 2004) and moderately-

905 uplifted (e.g. Granger et al., 1997; Anthony and Ganger, 2007) settings, or in river catchments marked
906 by enhanced glacial deepening (Haüselmann et al., 2007).

907 *6.2.2. Overcoming incomplete shielding: isochron burial dating of fill terraces*

908 The ≥30 m overburden thickness as a prerequisite for a complete shielding is unfortunately not often
909 met in cases of river terraces, even in thick fill terraces (Fig. 8d). In these instances, incomplete
910 shielding of the fluvial sediment to the cosmic rays may imply significant postburial production through
911 deeply-penetrating muons (Granger and Muzikar, 2001). As postburial production is very difficult to
912 constrain, it may become a considerable issue to produce reliable burial ages. This problem was
913 overcome by the isochron burial dating method (Balco and Rovey, 2008), which involves the sampling
914 of several pebbles from the same stratigraphical layer at the base of the river terrace (Erlanger et al.,
915 2012; Darling et al., 2013). It relies on the fact that these clasts are likely to have originated from
916 different source areas in the catchment (Erlanger et al., 2012). As the latter is subject to variable
917 production and/or surface erosion rates, and clasts have variable transport and/or storage time within
918 the fluvial system, they have distinct pre-burial histories resulting in different ^{10}Be and ^{26}Al inherited
919 concentrations. Sampling the same stratigraphical layer implies an identical postburial production for
920 each of them; this parameter can thus be treated as a constant among samples (Erlanger et al.,
921 2012). On the graphical representation of isochron burial dating (^{26}Al concentration plotted against
922 ^{10}Be concentration), the burial age is calculated from the slope of the regression line (Fig. 8e). Used
923 on a well-preserved terrace flight in South Africa (Sundays River), this approach yielded valuable
924 terrace ages for inferring Late Cenozoic incision rates (Erlanger et al., 2012).

925 *6.3. Future potential of TCN dating*

926 In addition to the commonly employed TCN (^{3}He, ^{10}Be, ^{21}Ne, ^{26}Al and ^{36}Cl), the use of further
927 radionuclides may extend the application time span of TCN. On the one hand, the long-lived ^{53}Mn
928 nuclide, given its half-life of 3.7±0.4 Ma, has the potential to unravel exposure histories older than 10
929 Ma in iron-bearing materials, although it requires AMS technologies with higher energies than those
930 presently attained in order to reduce the analytical uncertainty (Schäfer et al., 2006). On the other
931 hand, *in situ*-produced ^{14}C, with its short half-life, is able to reveal short-term sediment storage time
932 within large floodplains (Hippe et al., 2012). These values can be compared with long-term estimates
933 of sediment production when they are used in combination with ^{10}Be and ^{26}Al (Hippe et al., 2012).
934 Also, coupling ^{21}Ne concentrations with the nuclide pair ^{10}Be and ^{26}Al, all measured in the same

quartz-bearing material, improves both the accuracy and the time range of $^{26}Al/^{10}Be$ burial dating (Balco and Shuster, 2009).

7. Application of multiple numerical dating methods to single fluvial sequences

In this contribution, we have focused on the major recent developments of five numerical dating techniques and showed how these have enabled new dating applications in diverse fluvial settings at different time scales. However, two main recommendations must be borne in mind. First, there is no ideal numerical dating method that can provide accurate age results on any kind of sample and in any context. The use of a dating method, even the most established one such as ^{14}C, is limited by a range of intrinsic constraints and based on some implicit assumptions. Because the latter are rarely openly stated, expectations regarding numerical dating methods from non-geochronologists are sometimes unreasonable. Setting more realistic expectations from non-specialists is a key aim of this paper. Second, each method presented here, when applied to fluvial archives or landforms, may encounter specific methodological issues. This, in turn, may bias the "true" age of the event that has to be dated: for instance, age overestimation of a fluvial depositional event may be caused by the reworking of organic material (^{14}C), incomplete bleaching of the quartz dosimeter (OSL and ESR), inaccurate estimation of the initial ($^{230}Th/^{232}Th$) activity ratio ($^{230}Th/U$) or inherited nuclide concentrations (TCN).

To overcome some of these limitations, we therefore strongly recommend applying three different approaches. Each of these is exemplified by case studies, including a discussion how the combination of these dating methods may strengthen the chronological framework of fluvial archives. First, provided that the petrographic composition of the fluvial sediments is favourable, some of these dating methods may allow an internal cross-check. For instance, surface exposure ages are strengthened when ^{10}Be concentrations are measured alongside ^{36}Cl concentrations from quartz-bearing and calcite-bearing material, respectively (e.g. Le Dortz et al., 2011). The same holds for luminescence dating: Colarossi et al. (2015) comparatively analysed OSL (quartz) and post-IR IRSL (feldspar) signals from identical samples collected in Quaternary river sediments (South Africa) to test whether the second dosimeter can reliably date partially bleached sediments. Notwithstanding the statement that the post-IR $IRSL_{225}$ signal was the most adequate because of the fastest bleaching kinetics, age convergence and divergence were both observed for younger (<20 ka) and older (>50 ka) samples, respectively (Colarossi et al., 2015). Further research is however required to understand the cause(s) of this discrepancy for older fluvial material.

965 Second, as stated by Brauer et al. (2014), it is of major importance to produce independent
966 chronologies obtained from different dating methods, provided that the nature and the characteristics
967 of the fluvial deposits allows it (e.g. Table 1). A common combination involves radiocarbon and OSL
968 dating to yield robust chronologies for Late Pleistocene/Holocene fluvial sequences (e.g. de Moor et
969 al., 2008). Moreover, age discrepancies between these two dating methods may give further insights
970 into methodological issues. For instance, based on directly comparable paired OSL and ^{14}C ages of
971 Late Pleistocene terrace deposits from Eastern England, Briant and Bateman (2009) showed that
972 ages inferred from both methods are either consistent (<29-35 ka) or divergent (>29-35 ka) (Fig. 9a).
973 The systematic age underestimation of ^{14}C dating beyond this limit is attributed to secondary
974 contamination of older organic material by low levels of modern carbon (Fig. 3); it was thus suggested
975 that conventionally pre-treated ^{14}C ages ≥29 -35 ka should be treated with great caution (Briant and
976 Bateman, 2009). Likewise, some of the case studies mentioned in this contribution take advantage of
977 rarely used combinations between OSL, ESR, $^{230}Th/U$ and TCN dating (Chaussé et al., 2004; Stock et
978 al., 2005; Kock et al., 2009; Le Dortz et al., 2011; Blisniuk et al. 2012). For instance, Blisniuk et al.
979 (2012) applied a combination of ^{10}Be exposure dating with $^{230}Th/U$-dating to constrain the deposition of
980 mid-Holocene to late Pleistocene alluvial fans (California). Three sampling strategies were
981 implemented for the first method: top surface of individual large boulders (Fig. 7a), amalgamate of
982 surface clasts and depth profile (Fig. 7c). The second method involved the sampling of post-
983 depositional pedogenic carbonate from sub-surface clast-coatings. $^{230}Th/U$ ages (minimum ages) are
984 convergent or slightly younger than TCN ages (maximum ages if not corrected for inheritance and
985 assuming zero denudation), thereby proving the usefulness of this combined approach in obtaining
986 reliable depositional ages of fan deposits (Fig. 9b). Furthermore, the computing of ^{10}Be depth profile
987 ages of Late Pleistocene alluvium was made easier by the valuable minimum age information inferred
988 from $^{230}Th/U$ dating (Fig. 9b).

989 Third, as well as the parallel use of two or more independent methods from the same fluvial
990 sequences, a few exploratory studies have attempted to merge the dating principles of distinct
991 methods. For instance, Guralnik et al. (2011) developed an innovative approach using a mathematical
992 framework for consistently incorporating ^{10}Be concentration data along a depth profile with OSL ages
993 from a single alluvial section (Fig. 9c, d). This model is based on three parameters and solves an
994 integrated, co-dependent and self-consistent set of equations and assumes fluvial aggradation at a
995 constant rate, with uniform cosmogenic inheritance, followed by terrace abandonment and subsequent

preservation and exposure of its surface (Fig. 9c, d). This scenario of terrace evolution may be validated or rejected by comparing model depth concentration data and model OSL ages to real observations (Guralnik et al., 2011).

As a conclusion, establishing reliable chronologies for Quaternary fluvial sequences has strongly benefited from such applications of multiple dating methods. We finally recommend combining age results of numerical methods with chronological information obtained from relative dating methods. This is particularly well exemplified by the study of Antoine et al. (2007), synthesizing age results in the Somme valley (northern France), where diverse numerical (^{14}C, TL, IRSL, ESR, ^{230}Th/U) and relative (palaeomagnetism, mammalian biostratigraphy and amino-acid racemization) methods were implemented. In addition, control for ESR dating was internally provided by cross-checking results of optically bleached quartz grains with U-series/ESR dating of tooth enamel. This multi-dating approach enabled Antoine et al. (2007) to build a coherent and robust chronostratigraphical interpretation of the terrace sequence of the Somme valley for the last 1 Ma.

Acknowledgements

M. Duval's research was funded by a Marie Curie International Outgoing Fellowship of the EU's Seventh Framework Programme (FP7/2007-2013), awarded under REA Grant Agreement No. PIOF-GA-2013-626474. D. Scholz acknowledges funding of the DFG (SCHO 1274/9-1). Two anonymous reviewers are acknowledged for their thoughtful suggestions on an earlier version of this manuscript. David Bridgland is also acknowledged for his editorial work and for having improved the English of the manuscript.

References

Adams, K.D., Locke, W.W., Rossi, R., 1992. Obsidian-hydration dating of fluvially reworked sediments in the West Yellowstone region, Montana. Quaternary Research 38, 180-195.

Adamson, K.R., Woodward, J.C., Hughes, P.D., 2014. Glaciers and rivers: Pleistocene uncoupling in a Mediterranean mountain karst. Quaternary Science Reviews 94, 28-43.

Aitken, M.J. 1985. *Thermoluminescence dating.* Academic Press, London.

Anderson, R.S., Repka, J.L., Dick, G.S., 1996. Explicit treatment of inheritance in dating depositional surfaces using in situ ^{10}Be and ^{26}Al. Geology 24, 47–51.

Anthony, D.M., Granger, D.E., 2007. A new chronology for the age of Appalachian erosional surfaces determined by cosmogenic nuclides in cave sediments. Earth Surface Process and Landforms 887, 874–887.

1027 Antoine, P., Limondin Lozouet, N., Chaussé, C., Lautridou, J.-P., Pastre, J.-F., Auguste, P., Bahain, J.-J.,
1028 Falguères, C., Galehb, B., 2007. Pleistocene fluvial terraces from northern France (Seine, Yonne, Somme):
1029 synthesis, and new results from interglacial deposits. Quaternary Science Reviews 26(22–24), 2701-2723.
1030 Antón, L., Rodés, A., De Vicente, G., Pallàs, R., Garcia-Castellanos, D., Stuart, F.M., Braucher, R., Bourlès, D.,
1031 2012. Quantification of fluvial incision in the Duero Basin (NW Iberia) from longitudinal profile analysis and
1032 terrestrial cosmogenic nuclide concentrations. Geomorphology 165-166, 50–61.
1033 Arnold, L.J., Roberts, R.G., 2009. Stochastic modelling of multi-grain equivalent dose (De) distributions:
1034 implications for OSL dating of sediment mixtures. Quaternary Science Reviews 4, 209-230.
1035 Arnold, L.J., Demurob, M., Parésc, J.M., Pérez-Gonzálezc, A., Arsuagad, J.L., Bermúdez de Castroc, J.M.,
1036 Carbonell, E., 2015. Evaluating the suitability of extended-range luminescence dating techniques over early and
1037 Middle Pleistocene timescales: Published datasets and case studies from Atapuerca, Spain. Quaternary
1038 International 389, 167–190.
1039 Balco, G., Rovey, C.W., 2008. An isochron method for cosmogenic-nuclide dating of buried soils and sediments.
1040 American Journal of Science 308, 1083–1114.
1041 Balco, G., Shuster, D.L., 2009. ^{26}Al-^{10}Be-^{21}Ne burial dating. Earth and Planetary Science Letters 286, 570–575.
1042 Bartz, M., Klasen, N., Zander, A., Brill, D., Rixhon, G., Seeliger, M., Eiwanger, J., Weniger, G.-C., Mikdad, A.,
1043 Brückner, H., 2015.. Luminescence dating of ephemeral stream deposits around the Palaeolithic site of Ifri
1044 n'Ammar (Morocco). Quaternary Geochronology 30, 460-465.
1045 Bates, M.R., 1994. Quaternry aminostratigraphy in northwestern France. Quaternary Science Reviews 12, 793–
1046 809.
1047 Baynes, E.R.C., Attal, M., Niedermann, S., Kirstein, L.A., Dugmore, A.J., Naylor, M., 2015. Erosion during
1048 extreme flood events dominates Holocene canyon evolution in northeast Iceland. Proceedings of the National
1049 Academy of Sciences 112, 2355-2360.
1050 Beerten, K., Stesmans, A., 2006. Some properties of Ti-related paramagnetic centres relevant for electron spin
1051 resonance dating of single sedimentary quartz grains. Applied Radiation and Isotopes 64, 594-602.
1052 Bird, M.I., Ayliffe, L.K., Fifield, L.K., Turney, C.M., Cresswell, R.G., Barrows, T.T., David, B., 1999. Radiocarbon
1053 dating of" old" charcoal using a wet oxidation, stepped-combustion procedure. Radiocarbon 41, 127-140.
1054 Bischoff, J.L., Fitzpatrick, J.A., 1991. U-series dating of impure carbonates: An isochron technique using total-
1055 sample dissolution. Geochimica et Cosmochimica Acta 55, 543-554.
1056 Blisniuk, K., Oskin, M., Fletcher, K., Rockwell, T., Sharp, W., 2012. Assessing the reliability of U-series and ^{10}Be
1057 dating techniques on alluvial fans in the Anza Borrego Desert, California. Quaternary Geochronology 13, 26-41.
1058 Blisniuk, P.M. and Sharp, W.D., 2003. Rates of late Quaternary normal faulting in central Tibet from U-series
1059 dating of pedogenic carbonate in displaced fluvial gravel deposits. Earth and Planetary Science Letters 215, 169-
1060 186.

1061 Bourdon, B., Henderson, G.M., Lundstrom, C.C., Turner, S.P. (Eds.), 2003. Uranium-series Geochemistry.
1062 Mineralogical Society of America, Washington, DC.
1063 Braucher, R., Del Castillo, P., Siame, L., Hidy, A.J., Bourlès, D.L., 2009. Determination of both exposure time and
1064 denudation rate from an in situ-produced 10Be depth profile: A mathematical proof of uniqueness. Model
1065 sensitivity and applications to natural cases. Quaternary Geochronology 4, 56–67.
1066 Brauer, A., Hajdas, I., Blockley, S.P., Ramsey, C.B., Christl, M., Ivy-Ochs, S., Moseley, G.E., Nowaczyk, N.N.,
1067 Rasmussen, S.O., Roberts, H.M., Spötl, C., 2014. The importance of independent chronology in integrating
1068 records of past climate change for the 60–8 ka INTIMATE time interval. Quaternary Science Reviews 106, 47-66.
1069 Briant, R.M., Coope, G.R., Preece, R.C., Gibbard, P.L., 2004. Evidence for early Devensian (Weichselian) fluvial
1070 sedimentation: Geochronological and palaeoenvironmental data from the Upper Pleistocene deposits at Deeping
1071 St James, Lincolnshire, England. Quaternaire 15, 5–15.
1072 Briant, R.M., Bates, M.R., Schwenninger, J-L., Wenban-Smith, F.F. 2006. A long optically-stimulated
1073 luminescence dated Middle to Late Pleistocene fluvial sequence from the western Solent Basin, southern
1074 England. Journal of Quaternary Science 21, 507-523.
1075 Briant, R.M., Bateman, M.D., 2009. Luminescence dating indicates radiocarbon age underestimation in late
1076 Pleistocene fluvial deposits from eastern England. Journal of Quaternary Science 24, 916-927.
1077 Brock, F., Higham, T., Ditchfield, P., Bronk Ramsey, C., 2010. Current pretreatment methods for AMS
1078 radiocarbon dating at the Oxford Radiocarbon Accelerator Unit (ORAU). Radiocarbon 52, 103-112.
1079 Broecker, W.S., 1963. A preliminary evaluation of uranium series inequilibrium as a tool for absolute age
1080 measurement on marine carbonates. Journal of Geophysical Research 68, 2817-2834.
1081 Brunnacker, K., Löscher, M., Tillmanns, W., Urban, B., 1982. Correlation of the Quaternary terrace sequence in
1082 the lower Rhine Valley and northern Alpine foothills of Central Europe. Quaternary Research 18, 152–173.
1083 Burbank D.W., Leland, J., Fielding, E., Anderson, R.S., Brozovic, N., Reid, M.R., Duncan, C., 1996. Bedrock
1084 incision, rock uplift & threshold hillsopes in NW Himalayas. Nature 379, 505–510.
1085 Buylaert, J.P., Murray, A.S., Thomsen, K.J., Jain, M., 2009. Testing the potential of an elevated temperature
1086 IRSL signal from K-feldspar. Radiation Measurements 44, 560-565.
1087 Candy, I., Black, S., Sellwood, B.W., 2004. Quantifying time scales of pedogenic calcrete formation using U-
1088 series disequilibria. Sedimentary Geology 170, 177-187.
1089 Candy, I., Black, S., Sellwood, B.W., 2005. U-series isochron dating of immature and mature calcretes as a basis
1090 for constructing Quaternary landform chronologies for the Sorbas basin, southeast Spain. Quaternary Research
1091 64, 100-111.
1092 Candy, I., Schreve, D., 2007. Land-sea correlation of Middle Pleistocene temperate sub-stages using high-
1093 precision uranium-series dating of tufa deposits from southern England. Quaternary Science Reviews 26, 1223-
1094 1235.

1095 Chaussé, C., Voinchet, P., Bahain, J.J., Connet, N., Lhomme, V., Limondin-Lozouet, N., 2004. Middle and upper
1096 Pleistocene evolution of the river Yonne valley (France). Quaternaire 15, 53–64.
1097 Cheng, H., Edwards, R.L., Hoff, J., Gallup, C.D., Richards, D.A., Asmerom, Y., 2000. The half-lives of uranium-
1098 234 and thorium-230. Chemical Geology 169, 17-33.
1099 Cheng, H., Edwards, R.L., Shen, C.-C., Polyak, V.J., Asmerom, Y., Woodhead, J., Hellstrom, J., Wang, Y., Kong,
1100 X., Spötl, C., Wang, X., Alexander Jr., E.C., 2013. Improvements in ^{230}Th dating, ^{230}Th and ^{234}U half-life values,
1101 and U-Th isotopic measurements by multi-collector inductively coupled plasma mass spectrometry. Earth and
1102 Planetary Science Letters 371, 82-91.
1103 Colarossi D., Duller G.A.T., Roberts H.M., Tooth S., Lyons R., 2015. Comparison of paired quartz OSL and
1104 feldspar post-IR IRSL dose distributions in poorly bleached fluvial sediments from South Africa. Quaternary
1105 Geochronology 30, 233-238.
1106 Colman, S.M., Pierce, K.L., 1981. Weathering rinds on andesitic and basaltic stones as a Quaternary Age
1107 indicator, Western United States. Geological Survey Professional Paper 1210 1–56.
1108 Coltorti, M., Della Fazia, J., Paredes Rios, F., Tito, G., 2010. The Nuagapua alluvial fan sequence: Early and Late
1109 Holocene human-induced changes in the Bolivian Chaco? Proceedings of the Geologists' Association 121, 218–
1110 228.
1111 Cordier, S., Harmand, D., Lauer, T., Voinchet, P., Bahain, J.-J., Frechen, M., 2012. Geochronological
1112 reconstruction of the Pleistocene evolution of the Sarre valley (France and Germany) using OSL and ESR dating
1113 techniques. Geomorphology 165–166, 91-106.
1114 Cordier, S., Frechen, M., Harmand, D., 2014. Dating fluvial erosion: Fluvial response to climate change in the
1115 Moselle catchment (France, Germany) since the Late Saalian. Boreas 43, 450–468.
1116 Crook, R., 1986. Relative dating of Quaternary deposits based on P-wave velocities in weathered granitic clasts.
1117 Quaternary Research 25, 281–292.
1118 Cunha, P.P., Almeida, N.A.C., Aubry, T., Martins, A.A., Murray, A.S., Buylaert, J.P., Sohbati, R., Raposo, L.,
1119 Rocha, L., 2012. Records of human occupation from Pleistocene river terrace and aeolian sediments in the
1120 Arneiro depression (Lower Tejo River, central eastern Portugal). Geomorphology 165-166, 78–90.
1121 Cunningham, A.C., Wallinga, J., 2010. Selection of integration time intervals for quartz OSL decay
1122 curves. Quaternary Geochronology 5, 657-666.
1123 Cunningham A.C., Wallinga, J., 2012. Realizing the potential of fluvial archives using robust OSL chronologies.
1124 Quaternary Geochronology 12, 98-106.
1125 Darling, A.L., Karlstrom, K.E., Granger, D.E., Aslan, A., Kirby, E., Ouimet, W.B., Lazear, G.D., Coblentz, D.D.,
1126 Cole, R.D., 2012. New incision rates along the Colorado River system based on cosmogenic burial dating of
1127 terraces: Implications for regional controls on Quaternary incision. Geosphere 8, 1020–1041.
1128 Davis, W.M., 1899. The geographical cycle. Geogr. J. 481–504.
1129 Davis, R., Schaeffer, O.A., 1955. Chlorine-36 in nature. Ann. NY Acad. Sc. 62, 105-122.

Deevey Jr, E.S., Gross, M.S., Hutchinson, G.E. and Kraybill, H.L., 1954. The natural C14 contents of materials from hard-water lakes. Proceedings of the National Academy of Sciences 40, 285.

de Moor, J.J.W., Kasse, C., van Balen, R., Vandenberghe, J., Wallinga, J., 2008. Human and climate impact on catchment development during the Holocene - Geul River, the Netherlands. Geomorphology 98, 316–339.

Despriée, J., Gageonnet, R., Voinchet, P., Bahain, J.J., Falguères, C., Duvialard, J., Varache, F., 2004. Pleistocene fluvial systems of the Creuse River (Middle Loire Basin - Centre Region, France). Quaternaire 15, 77–86.

Ditlefsen, C., 1992. Bleaching of K-feldspars in turbid water suspensions: A comparison of photo- and thermoluminescence signals. Quaternary Science Reviews 11, 33-38.

Dunai, T., 2010. Cosmogenic nuclides - Principles, Concepts and Applications in the Earth Surface Sciences, Cambridge University Press, 187p.

Duller, G.A.T., 2004. Luminescence dating of Quaternary sediments: recent advances. Journal of Quaternary Science 19, 183-192.

Duller, G.A.T., 2008. Single-grain optical dating of Quaternary sediments: why aliquot size matters in luminescence dating. Boreas 37, 589-612.

Duval, M., 2012. Dose response curve of the ESR signal of the Aluminum center in quartz grains extracted from sediment. Ancient TL 30, 1-9.

Duval, M., 2015. Electron Spin Resonance (ESR) Dating of Fossil Tooth Enamel. Encyclopedia of Scientific Dating Methods. W. J. Rink and J. W. Thompson, Springer Netherlands, 239-246.

Duval., M. (2016). Electron Spin Resonance Dating in Archaeology. In: Gilbert A.S. (Ed.) *Encyclopedia of Geoarchaeology*. Springer. DOI: 10.1007/978-1-4020-4409-0.

Duval, M., Guilarte Moreno, V., 2012. Assessing the influence of the cavity temperature on the ESR signal of the Aluminum center in quartz grains extracted from sediment. Ancient TL 30, 11-16.

Duval, M, Guilarte V., 2012. ESR dosimetry of optically bleached quartz grains extracted from Plio-Quaternary sediment: Evaluating some key aspects of the ESR signals associated to the Ti-centers. Radiation Measurements 78, 28-41.

Duval, M., Sancho, C., Calle, M., Guilarte, V., Peña-Monné, J.L., 2015. On the interest of using the multiple center approach in ESR dating of optically bleached quartz grains: Some examples from the Early Pleistocene terraces of the Alcanadre River (Ebro basin, Spain). Quaternary Geochronology 29, 58-69.

Edwards, R.L., Chen, J.H., Wasserburg, G. J., 1987. ^{238}U-^{234}U-^{230}Th-^{232}Th systematics and the precise measurement of time over the past 500,000 years. Earth and Planetary Science Letters 81, 175-192.

Edwards, R.L., Gallup, C.D., Cheng, H., 2003. Uranium-series dating of marine and lacustrine carbonates. In: Bourdon, B., Henderson, G.M., Lundstrom, C.C., and Turner, S. P. Eds.), *Uranium-series Geochemistry*. Mineralogical Society of America, Washington, DC.

1164 Eggins, S.M., Grün, R., McCulloch, M.T., Pike, A.W.G., Chappell, J., Kinsley, L., Mortimer, G., Shelley, M.,
1165 Murray-Wallace, C.V., Spötl, C., Taylor, L., 2005. In situ U-series dating by laser-ablation multi-collector ICPMS:
1166 new prospects for Quaternary geochronology. Quaternary Science Reviews 24, 2523-2538.
1167 Engel, S.A., Gardner, T.W., Ciolkosz, E.J., 1996. Quaternary soil chronosequences on terraces of the
1168 Susquehanna River, Pennsylvania. Geomorphology 17, 273–294.
1169 Erlanger, E.D., Granger, D.E., Gibbon, R.J., 2012. Rock uplift rates in South Africa from isochron burial dating of
1170 fluvial and marine terraces. Geology 40, 1019–1022.
1171 Falguères, C., Bahain, J.-J., Pérez-González, A., Mercier, N., Santonja, M., Dolo, J.-M., 2006. The Lower
1172 Acheulian site of Ambrona, Soria (Spain): ages derived from a combined ESR/U-series model. Journal of
1173 Archaeological Science 33, 149-157.
1174 Flez, C., Lahousse, P., 2015. Example of Holocene alpine torrent response to environmental change : contribution
1175 to assessment of forcing factors. Quaternaire 15, 167–176.
1176 Fontana, A., Mozzi, P., Bondesan, A., 2008. Alluvial megafans in the Venetian-Friulian Plain (north-eastern Italy):
1177 Evidence of sedimentary and erosive phases during Late Pleistocene and Holocene. Quaternary International
1178 189, 71–90.
1179 Fuchs, M.C., Kreutzer, S., Burow, C., Dietze, M., Fischer, M., Schmidt, C., Fuchs, M., 2015. Data processing in
1180 luminescence dating analysis: An exemplary workflow using the R package 'Luminescence'. Quaternary
1181 International 362, 8-13.
1182 Galbraith, R.F., 2010. On plotting OSL equivalent dose estimates. Ancient TL 28, 1-9.
1183 Galbraith, R.F., Green, P.F., 1990. Estimating the component ages in a finite mixture. Nuclear Tracks and
1184 Radiation Measurements 17, 197-206.
1185 Galbraith, R.F., Laslett, G.M., 1993. Statistical models for mixed fission track ages. Nuclear Tracks and Radiation
1186 Measurements 21, 495-470.
1187 Galbraith, R.F., Roberts, R.G., 2012. Statistical aspects of equivalent dose and error calculation and display in
1188 OSL dating: an overview and some recommendations. Quaternary Geochronology 11, 1-27.
1189 Garnier, A., Lespez, L., Ozainne, S., Ballouche, A., Mayor, A., Le Drézen, Y., Rasse, M., Huysecom, E., 2015.
1190 L'incision généralisée de la vallée du Yamé (Mali) entre 2 350 et 1 700 ans cal. BP : quelle signification
1191 paléoenvironnementale et archéologique? Quaternaire 26, 49-66.
1192 Geach, M.R., Thomsen, K.J., Buylaert, J.-P., Murray, A.S., Mather, A.E., Telfer, M.W., Stokes, M., 2015. Single-
1193 grain and multi-grain OSL dating of river terrace sediments in the Tabernas Basin, SE Spain. Quaternary
1194 Geochronology 30, 213-218
1195 Godwin, H., 1962. Half-life of radiocarbon. Nature 195.
1196 Goldstein, S.J., Stirling, C.H., 2003. Techniques for measuring Uranium-series nuclides: 1992-2002. In: Bourdon,
1197 B., Henderson, G.M., Lundstrom, C.C., and Turner, S.P. Eds.), *Uranium-series Geochemistry*. Mineralogical
1198 Society of America, Washington, DC.

1199 Gosse, J.C., Phillips, F.M., 2001. Terrestrial in situ cosmogenic nuclides: theory and application. Quaternary
1200 Science Reviews 20, 1475–1560.
1201 Gorter, S.C., 1936. Paramagnetic relaxation in a transversal magnetic field. Physica 3, 1006–1008.
1202 Granger, D.E., Kirchner, J.W., Finkel, R.C., 1997. Quaternary downcutting rate of the New River, Virginia,
1203 measured from differential decay of cosmogenic ^{26}Al and ^{10}Be in cave-deposited alluvium. Geology 25, 107–110.
1204 Granger, D.E., Muzikar, P.F., 2001. Dating sediment burial with in situ-produced cosmogenic nuclides: theory,
1205 techniques, and limitations. Earth and Planetary Science Letters 188, 269–281.
1206 Granger, D.E., 2014. Cosmogenic Nuclide Burial Dating in Archaeology and Paleoanthropology, in: Treatise on
1207 Geochemistry: Second Edition. Elsevier Ltd., pp. 81–97.
1208 Grün, R., 1989. Electron spin resonance (ESR) dating. Quaternary International 1(0), 65-109.
1209 Grün, R., 2000. An alternative model for open system U-series/ESR age calculations: (closed system U-series)-
1210 ESR, CSUS-ESR. Ancient TL 18(1), 1-4.
1211 Grün, R., 2009. The relevance of parametric U-uptake models in ESR age calculations. Radiation Measurements
1212 44(5–6), 472-476.
1213 Grün, R., Schwarcz, H.P., Chadam, J., 1988. ESR dating of tooth enamel: Coupled correction for U-uptake and
1214 U-series disequilibrium. Nuclear Tracks and Radiation Measurements 14, 237-241
1215 Guerin, G., Combès, B., Lahaye, C., Thomsen, K.J., Tribolo, C., Urbanova, P., Guibert, P., Mercier, N., Valladas,
1216 H., 2015. Testing the accuracy of a Bayesian central-dose model for single-grain OSL, using known-age samples.
1217 Radiation Measurements 81, 62-70.
1218 Guilarte, V., Trompier, F., Duval, M**.** Evaluating the potential of Q-band ESR spectroscopy for dose reconstruction
1219 of fossil tooth enamel. *PLoS ONE* 11(3): e0150346. DOI:10.1371/journal.pone.0150346.
1220 Guralnik, B., Matmon, A., Avni, Y., Porat, N., Fink, D., 2011. Constraining the evolution of river terraces with
1221 integrated OSL and cosmogenic nuclide data. Quaternary Geochronology 6, 22–32.
1222 Harmand, D., Voinchet, P., Cordier, S., Bahain, J., Rixhon, G., 2015. Datations ESR de terrasses alluviales des
1223 vallées de la Moselle et de la Meurthe (France, Allemagne): implications chronostratigraphiques et limites
1224 méthodologiques. Quaternaire, 13–26.
1225 Häuselmann, P., Granger, D.E., Jeannin, P.-Y., Lauritzen, S.-E., 2007. Abrupt glacial valley incision at 0.8 Ma
1226 dated from cave deposits in Switzerland. Geology 35, 143–146.
1227 Hellstrom, J.C., 2006. U-Th dating of speleothems with high initial ^{230}Th using stratigraphical constraint.
1228 Quaternary Geochronology 1, 289-295.
1229 Hidy, A.J., Gosse, J.C., Pederson, J.L., Mattern, J.P., Finkel, R.C., 2010. A geologically constrained Monte Carlo
1230 approach to modeling exposure ages from profiles of cosmogenic nuclides: An example from Lees Ferry, Arizona.
1231 Geochemistry, Geophysics, Geosystems 11.
1232 Higham, T.F., Jacobi, R.M., Ramsey, C.B., 2006. AMS radiocarbon dating of ancient bone using ultrafiltration.
1233 Radiocarbon 48, 179.

1234 Hippe, K., Kober, F., Zeilinger, G., Ivy-Ochs, S., Maden, C., Wacker, L., Kubik, P.W., Wieler, R., 2012.
1235 Quantifying denudation rates and sediment storage on the eastern Altiplano, Bolivia, using cosmogenic ^{10}Be, ^{26}Al,
1236 and *in situ* ^{14}C. Geomorphology 179, 58–70.
1237 Hogg, A.G., Hua, Q., Blackwell, P.G., Niu, M., Buck, C.E., Guilderson, T.P., Heaton, T.J., Palmer, J.G., Reimer,
1238 P.J., Reimer, R.W., Turney, C.S., 2013. SHCal13 Southern Hemisphere calibration, 0–50,000 years cal BP.
1239 Radiocarbon 55, 1889-1903.
1240 Huntley, D.J., Godfrey-Smith, D.I., Thewalt, M.L., 1985. Optical dating of sediments. Nature 313, 105-107.
1241 Huntley, D.J., Lamothe, M., 2001. Ubiquity of anomalous fading in K-feldspars and the measurement and
1242 correction for it in optical dating. Canadian Journal of Earth Sciences 38, 1093-1106.
1243 Ikeya, M., 1975. Dating a stalactite by electron paramagnetic resonance. Nature 255, 48-50.
1244 Ikeya, M., 1993. New Applications of Electron Spin Resonance Dating, Dosimetry and Microscopy. Singapore,
1245 World Scientific.
1246 Ivanovich, M., & Harmon, R. S. (Eds.). (1992). *Uranium-series disequilibrium: Applications to earth, marine, and*
1247 *environmental sciences*. Oxford University Press.
1248 Ivy-Ochs, S, Kober, F., 2008. Surface exposure dating with cosmogenic nuclides. Eiszeitalter und Gegenwart –
1249 Quaternary Science Journal 57, 179-209.
1250 Jacobson, R.B., Elston, D.P., Heaton, J.W., 1988. Stratigraphy and magnetic polarity of the High Terrace
1251 remnants in the Upper Ohio and Monongahela Rivers in West Virginia, Pennsylvania and Ohio. Quaternary
1252 Research 29, 216–232.
1253 Jain, M., Murray, A.S., Botter-Jensen, L., 2004. Optically stimulated luminescence dating: How significant is
1254 incomplete light exposure in fluvial environments? Quaternaire 15, 143–157.
1255 Jain, M., Murray, A.S., Bøtter-Jensen, L., Wintle, A.G., 2005. A single-aliquot regenerative-dose method based on
1256 IR bleaching of the fast OSL component in quartz. Radiation Measurements 39, 309-318.
1257 Joannes-Boyau, R.,Grün, R., 2011. A comprehensive model for CO_2^- radicals in fossil tooth enamel: Implications
1258 for ESR dating. Quaternary Geochronology 6, 82-97.
1259 Kalicki, T., Sauchyk, S., Calderoni, G., Simakova, G., 2008. Climatic versus human impact on the Holocene
1260 sedimentation in river valleys of different order: Examples from the upper Dnieper basin, Belarus. Quaternary
1261 International 189, 91–105.
1262 Kasse, C., Bohncke, S.J.P., Vandenberghe, J., 1995. Fluvial periglacial environments, climate and vegetation
1263 during the Middle Weichselian in the Northern Netherlands with special reference to the Hengelo Interstadial.
1264 Mededelingen Rijks Geologische Dienst 52, 387-414.
1265 Kasse, C., Bohncke, S.J.P., Vandenberghe, J., Gábris, G., 2010. Fluvial style changes during the last glacial-
1266 interglacial transition in the middle Tisza valley (Hungary). Proceedings of the Geologists' Association 121, 180–
1267 194.

Kaufman, A., 1993. An evaluation of several methods for determining ^{230}Th/U ages in impure carbonates. Geochimica et Cosmochimica Acta 57, 2303-2317.

Kaufman, A., Broecker, W., 1965. Comparison of ^{230}Th and ^{14}C ages for carbonate materials from Lakes Lahontan and Bonneville. Journal of Geophysical Research 70, 4039-4054.

Keen-Zebert, A., Tooth, S., Rodnight, H., Duller, G.A.T., Roberts, H.M., Grenfell, M., 2013. Late Quaternary floodplain reworking and the preservation of alluvial sedimentary archives in unconfined and confined river valleys in the eastern interior of South Africa. Geomorphology 185, 54-66

Kelly, M., Black, S., Rowan, J.S., 2000. A calcrete-based U/Th chronology for landform evolution in the Sorbas basin, southeast Spain. Quaternary Science Reviews 19, 995-1010.

Klein, J., Middleton, R., Tang, H., 1982. Modifications of an FN tandem for quantitative ^{10}Be Measurement. Nuclear Instruments and Methods in Physic Researchs 193, 601–616.

Knuepfer, P., 1988. Estimating ages of late Quaternary stream terraces from analysis of weathering rinds and soils. Geological Society of America Bulletin 100, 1224–1236.

Kock, S., Kramers, J.D., Preusser, F., Wetzel, A., 2009. Dating of Late Pleistocene terrace deposits of the River Rhine using Uranium series and luminescence methods: Potential and limitations. Quaternary Geochronology 4, 363-373.

Kong, P., Granger, D.E., Wu, F.Y., Caffee, M.W., Wang, Y.J., Zhao, X.T., Zheng, Y., 2009. Cosmogenic nuclide burial ages and provenance of the Xigeda paleo-lake: Implications for evolution of the Middle Yangtze River. Earth and Planetary Science Letters 278, 131–141.

Kreutzer, S., Schmidt, C., Fuchs, M. C., Dietze, M., Fischer, M., Fuchs, M., 2012. Introducing an R package for luminescence dating analysis. Ancient TL 30, 1-8.

Ku, T.-L., Liang, Z.-C., 1984. The dating of impure carbonates with decay-series isotopes. Nuclear Instruments and Methods in Physics Research 223, 563-571.

Kuzucuoglu, C., Fontugne, M., Mouralis, D., 2004. Holocene terraces in the middle Euphrates valley, between Halfeti and Karkemish (Gaziantep, Turkey). Quaternaire 15, 195–206.

Lauer, T., Frechen, M., Hoselmann, C., Tsukamoto, S., 2010. Fluvial aggradation phases in the Upper Rhine Graben-new insights by quartz OSL dating. Proceedings of the Geologists' Association 121, 154–161.

Le Dortz, K., Meyer, B., Sébrier, M., Braucher, R., Nazari, H., Benedetti, L., Fattahi, M., Bourlès, D., Foroutan, M., Siame, L., Rashidi, A., Bateman, M.D., 2011. Dating inset terraces and offset fans along the Dehshir Fault (Iran) combining cosmogenic and OSL methods. Geophysical Journal International 185, 1147–1174.

Leland, J., Reid, M.R., Burbank, D.W., Finkel, R., Caffee, M., 1998. Incision and differential bedrock uplift along the Indus River near Nanga Parbat, Pakistan Himalaya, from ^{10}Be and ^{26}Al exposure age dating of bedrock straths. Earth and Planetary Science Letters 154, 93–107.

Lewin, J., Macklin, M.G., 2003. Preservation potential for Late Quaternary river alluvium. Journal of Quaternary Science 18, 107-120.

1303 Lewin, J., Macklin, M.G., Johnstone, E., 2005. Interpreting alluvial archives: sedimentological factors in the British
1304 Holocene fluvial record. Quaternary Science Reviews 24, 1873-1889.
1305 Libby, W.F., Anderson, E.C., Arnold, J.R., 1949. Age determination by radiocarbon content: world-wide assay of
1306 natural radiocarbon. Science 109, 227-228.
1307 Liu, C.-R., Grün, R., 2011. Fluvio-mechanical resetting of the Al and Ti centres in quartz. Radiation
1308 Measurements 46(10): 1038-1042.
1309 Ludwig, K.R., 2003. Mathematical-statistical treatment of data and errors for ^{230}Th/U geochronology. In: Bourdon,
1310 B., Henderson, G.M., Lundstrom, C.C., and Turner, S.P. Eds.), *Uranium-series Geochemistry*. Mineralogical
1311 Society of America, Washington, DC.
1312 Ludwig, K.R., Paces, J.B., 2002. Uranium-series dating of pedogenic silica and carbonate, Crater Flat, Nevada.
1313 Geochimica et Cosmochimica Acta 66, 487-506.
1314 Luo, S., Ku, T.-L., 1991. U-series isochron dating: A generalized method employing total-sample dissolution.
1315 Geochimica et Cosmochimica Acta 55, 555-564.
1316 Macklin, M.G., Johnstone, E., Lewin, J., 2005. Pervasive and long-term forcing of Holocene river instability and
1317 flooding in Great Britain by centennial-scale climate change. Holocene 15, 937-943.
1318 Macklin, M.G., Jones, A.F., Lewin, J., 2010. River response to rapid Holocene environmental change: evidence
1319 and explanation in British catchments. Quaternary Science Reviews 29, 1555-1576.
1320 Macklin, M.G., Lewin, J., 2003. River sediments, great floods and centennial-scale Holocene climate change.
1321 Journal of Quaternary Science 18, 101-105.
1322 Martin, L., Incerti, S., Mercier, N., 2015. DosiVox: Implementing Geant 4-based software for dosimetry simulations
1323 relevant to luminescence and ESR dating techniques. Ancient TL 33, 1-10.
1324 Martins, A.A., Cunha, P.P., Rosina, P., Osterbeek, L., Cura, S., Grimaldi, S., Gomes, J., Buylaert, J.P., Murray,
1325 A.S., Matos, J., 2010. Geoarchaeology of Pleistocene open-air sites in the Vila Nova da Barquinha-Santa Cita
1326 area (Lower Tejo River basin, central Portugal). Proceedings of the Geologists' Association 121, 128–140.
1327 Mathieu, J., Weisrock, A., Wengler, L., Brochier, J.E., Even, G., Fontugne, M., Mercier, N., Ouammou, A.,
1328 Sénégas, F., Valladas, H., Vernet, J.L., Wahl, L., 2015. Holocene deposits in the lower section of the Assaka
1329 Wadi, South Morocco: preliminary results. Quaternaire 15, 207–218.
1330 Mertz-Kraus, R., Jochum, K.P., Sharp, W.D., Stoll, B., Weis, U., Andreae, M.O., 2010. In situ ^{230}Th-^{232}Th-^{234}U-
1331 ^{238}U analysis of silicate glasses and carbonates using laser ablation single-collector sector-field ICP-MS. Journal
1332 of Analytical Atomic Spectrometry 25, 1895-1904.
1333 Millard, A., 2014. Conventions for reporting radiocarbon determinations. Radiocarbon 56, 555–559.
1334 Mol, J., Roebroeks, W., Kamermans, H., van Kolfschoten, T., Turq, A., 2004. Weichselian and holocene fluvial
1335 evolution of the Vézère river valley (Dordogne, France). Quaternaire 15, 187–193.
1336 Murray, A.S., Olley, J.M., 2002. Precision and accuracy in the optically stimulated luminescence dating of
1337 sedimentary quartz: a status review. Geochronometria 21, 1-16.

1338 Murray, A.S., Wintle, A.G., 2000. Luminescence dating of quartz using an improved single-aliquot regenerative-
1339 dose protocol. Radiation Measurements 32, 57-73.
1340 Murray, A.S., Wintle, A.G., 2003.The single aliquot regenerative dose protocol: potential for improvements in
1341 reliability. Radiation Measurements 37, 377-381.
1342 Nishiizumi, K., Lal, D., Klein, J., Middleton, R., Arnold, J., 1986. Production of ^{10}Be and ^{26}Al by cosmic rays in
1343 terrestrial quartz in situ and implications for erosion rates. Nature 319, 134-136.
1344 Owen, L. A., Clemmens, S.J., Finkel, R.C., Gray, H., 2014. Late Quaternary alluvial fans at the eastern end of the
1345 San Bernardino Mountains, Southern California. Quaternary Science Reviews 87, 114–134.
1346 Penkman, K.E.H., Preece, R.C., Keen, D.H., Maddy, D., Schreve, D.C., Collins, M.J., 2007. Testing the
1347 aminostratigraphy of fluvial archives: the evidence from intra-crystalline proteins within freshwater shells.
1348 Quaternary Science Reviews 26, 2958–2969.
1349 Philippsen, B., 2013. The freshwater reservoir effect in radiocarbon dating. Heritage Science 1, 24.
1350 Pigati, J.S., Quade, J., Wilson, J., Jull, A.T., Lifton, N.A., 2007. Development of low-background vacuum
1351 extraction and graphitization systems for ^{14}C dating of old (40–60 ka) samples. Quaternary International 166, 4-
1352 14.
1353 Preece, R.C., 1999. Mollusca from Last Interglacial fluvial deposits of the River Thames at Trafalgar Square,
1354 London. Journal of Quaternary Science 14, 77–89.
1355 Preusser, F., Chithambo, M.L., Götte, T., Martini, M., Ramseyer, K., Sendezera, E.J., Susino, G.J. and Wintle,
1356 A.G., 2009. Quartz as a natural luminescence dosimeter. Earth-Science Reviews 97, 184-214.
1357 Rades, E.F., Hetzel, R., Xu, Q., Ding, L., 2013. Constraining holocene lake-level highstands on the tibetan
1358 plateau by ^{10}Be exposure dating: A case study at tangra yumco, southern tibet. Quaternary Science Reviews 82,
1359 68–77.
1360 Ramos, A.M., Cunha, P.P., Cunha, L.S., Gomes, A., Lopes, F.C., Buylaert, J.P., Murray, A.S., 2012. The River
1361 Mondego terraces at the Figueira da Foz coastal area (western central Portugal): Geomorphological and
1362 sedimentological characterization of a terrace staircase affected by differential uplift and glacio-eustasy.
1363 Geomorphology 165-166, 107–123.
1364 Reimer, P.J., Baillie, M.G., Bard, E., Bayliss, A., Beck, J.W., Bertrand, C.J., Blackwell, P.G., Buck, C.E., Burr,
1365 G.S., Cutler, K.B., Damon, P.E., 2004. IntCal04 terrestrial radiocarbon age calibration, 0-26 cal kyr BP.
1366 Radiocarbon 46, 1029-1058.
1367 Reimer, P.J., Bard, E., Bayliss, A., Beck, J.W., Blackwell, P.G., Bronk Ramsey, C., Buck, C.E., Cheng, H.,
1368 Edwards, R.L., Friedrich, M., Grootes, P.M., 2013. IntCal13 and Marine13 Radiocarbon Age Calibration Curves
1369 0–50,000 Years cal BP. Radiocarbon 55, 1869-1887.
1370 Repka, J.L., Anderson, R.S., Finkel, R.C., 1997. Cosmogenic dating of fluvial terraces, Fremont River, Utah.
1371 Earth and Planetary Science Letters 152, 59–73.

1372 Reusser, L., Bierman, P., Pavich, M., Larsen, J., Finkel, R., 2006. An episode of rapid bedrock channel incision
1373 during the last glacial cycle, measured with ^{10}Be. American Journal of Science 306, 69–102.
1374 Richards, D.A., Dorale, J.A., 2003. Uranium-series chronology and environmental applications of speleothems. In:
1375 Bourdon, B., Henderson, G.M., Lundstrom, C.C., and Turner, S.P. Eds.), *Uranium-series Geochemistry*.
1376 Mineralogical Society of America, Washington, DC.
1377 Rink, W. J., Bartoll, J., Schwarcz, H.P., Shane, P., Bar-Yosef, O., 2007. Testing the reliability of ESR dating of
1378 optically exposed buried quartz sediments. Radiation Measurements 42, 1618-1626.
1379 Rittenour, T.M., 2008. Luminescence dating of fluvial deposits: applications to geomorphic, palaeoseismic and
1380 archaeological research. Boreas 37, 613-635.
1381 Rixhon, G., Braucher, R., Bourlès, D., Siame, L., Bovy, B., Demoulin, A., 2011. Quaternary river incision in NE
1382 Ardennes (Belgium) – Insights from ^{10}Be/^{26}Al dating of river terraces. Quaternary Geochronology 6, 273–284.
1383 Rixhon, G., Bourlès, D.L., Braucher, R., Siame, L., Cordy, J.M., Demoulin, A., 2014. ^{10}Be dating of the Main
1384 Terrace level in the Amblève valley (Ardennes, Belgium): New age constraint on the archaeological and
1385 palaeontological filling of the Belle-Roche palaeokarst. Boreas 43, 528–542.
1386 Rodnight, H., 2008. How many equivalent dose values are needed to obtain a reproducible distribution? Ancient
1387 TL 26, 3-10.
1388 Rogerson, R.J., Keen, D.H., Coope, G.R., Robinson, E., Dickson, J.H., Dickson, C.A., 1992. The fauna, flora and
1389 palaeoenvironmental significance of deposits beneath the low terrace of the River Great Ouse at Radwell,
1390 Bedfordshire, England. Proceedings of the Geologists' Association 103, 1-13.
1391 Roy-Barman, M. Pons-Branchu, E., 2016. Improved U-Th dating of carbonates with high initial ^{230}Th using
1392 stratigraphical and coevality constraints. Quaternary Geochronology 32, 29-39.
1393 Ruff, M., Szidat, S., Gäggeler, H.W., Suter, M., Synal, H.A., Wacker, L., 2010. Gaseous radiocarbon
1394 measurements of small samples. Nuclear Instruments and Methods in Physics Research Section B: Beam
1395 Interactions with Materials and Atoms 268, 790-794.
1396 Salvador, P.G., Berger, J.F., Gauthier, E., Vanniere, B., 2004. Holocene fluctuations of the Rhône River in the
1397 alluvial plain of the basses terres (Isère, Ain, France). Quaternaire 15, 177–186.
1398 Sanderson, D.C.W, Murphy, W., 2010. Using simple portable OSL measurements and laboratory characterisation
1399 to help understand complex and heterogeneous sediment sequences for luminescence dating. Quaternary
1400 Geochronology 5, 299–305.
1401 Santonja, M., Pérez-González, A., Domínguez-Rodrigo, M., Panera, J., Rubio-Jara, S., Sesé, C., Soto, E., Arnold,
1402 L. J., Duval, M., Demuro, M., Ortiz, J.E., de Torres, T., Mercier, N., Barba, R., Yravedra, J., 2014. The Middle
1403 Paleolithic site of Cuesta de la Bajada (Teruel, Spain): a perspective on the Acheulean and Middle Paleolithic
1404 technocomplexes in Europe. Journal of Archaeological Science 49, 556-571.

1405 Schaefer, J.M., Faestermann, T., Herzog, G.F., Knie, K., Korschinek, G., Masarik, J., Meier, A., Poutivtsev, M.,
1406 Rugel, G., Schlüchter, C., Serifiddin, F., Winckler, G., 2006. Terrestrial manganese-53 - A new monitor of Earth
1407 surface processes. Earth and Planetary Science Letters 251, 334–345.
1408 Scherbina, O. I. and Brik, A. B., 2000. Temperature stability of carbonate groups in tooth enamel. Applied
1409 Radiation and Isotopes 52, 1071-1075.
1410 Schmidt C., Kreutzer S., DeWitt R., Fuchs M., 2015. Radiofluorescence of quartz : a review. Quaternary
1411 Geochronology 27, 66-77.
1412 Schmidt, S., Hetzel, R., Kuhlmann, J., Mingorance, F., Ramos, V.A., 2011. A note of caution on the use of
1413 boulders for exposure dating of depositional surfaces. Earth and Planetary Science Letters 302, 60–70.
1414 Scholz, D., Hoffmann, D.L., 2008. ^{230}Th/U-dating of fossil reef corals and speleothems. Eiszeitalter und
1415 Gegenwart – Quaternary Science Journal 57, 52-77.
1416 Schramm, A., Stein, M., Goldstein, S.L., 2000. Calibration of the ^{14}C time scale to >40 ka by ^{234}U-^{230}Th dating of
1417 Lake Lisan sediments (last glacial Dead Sea). Earth and Planetary Science Letters 175, 27-40.
1418 Schreve, D.C., 2001. Differentiation of the British late Middle Pleistocene interglacials: the evidence from
1419 mammalian biostratigraphy. Quaternary Science Reviews 20, 1693-1705.
1420 Schreve, D.C., Keen, D.H., Limondin-Lozouet, N., Auguste, P., Santistebane, J.I., Ubilla, M., Matoshko, A.,
1421 Bridgland, D.R., Westaway, R., 2007. Progress in faunal correlation of Late Cenozoic fluvial sequences 2000–4:
1422 the report of the IGCP 449 biostratigraphy subgroup. Quaternary Science Reviews 26, 2970-2995.
1423 Schulte, L., Julià, R., Burjachs, F., Hilgers, A., 2008. Middle Pleistocene to Holocene geochronology of the River
1424 Aguas terrace sequence (Iberian Peninsula): Fluvial response to Mediterranean environmental change.
1425 Geomorphology 98, 13-33.
1426 Schwarcz, H.P., 1989. Uranium series dating of Quaternary deposits. Quaternary International 1, 7-17.
1427 Schwarcz, H.P., Latham, A. G., 1989. Dirty calcites 1. Uranium-series dating of contaminated calcite using
1428 leachates alone. Chemical Geology 80, 35-43.
1429 Sharp, W.D., Ludwig, K.R., Chadwick, O.A., Amundson, R., Glaser, L.L., 2003. Dating fluvial terraces by ^{230}Th/U
1430 on pedogenic carbonate, Wind River Basin, Wyoming. Quaternary Research 59, 139-150.
1431 Siame, L.L., Bourlès, D.L., Sébrier, M., Bellier, O., Carlos Castano, J., Araujo, M., Perez, M., Raisbeck, G.M.,
1432 Yiou, F., 1997. Cosmogenic dating ranging from 20 to 700 ka of a series of alluvial fan surfaces affected by the El
1433 Tigre fault, Argentina. Geology 25, 975-978.
1434 Singareya, J.S., Bailey, R.M., 2004. Component-resolved bleaching spectra of quartz optically stimulated
1435 luminescence: preliminary results and implications for dating. Radiation Measurements 38, 111–118.
1436 Stock, G.M., Anderson, R.S., Finkel, R.C., 2004. Pace of landscape evolution in the Sierra Nevada, California,
1437 revealed by cosmogenic dating of cave sediments. Geology 32, 193-196.
1438 Stokes, S., Bray, H.E., Blum, M.D., 2001. Optical resetting in large drainage basins: tests of zeroing assumptions
1439 using single-aliquot procedures. Quaternary Science Reviews 20, 879-885.

Stone, A.E.C., Bateman, M.D., Thomas, D.S.G., 2015. Rapid age assessment in the Namib Sand Sea using a portable luminescence reader. Quaternary Geochronology 30, 134-140.

Stuiver, M., Polach, H.A., 1977. Discussion; reporting of C-14 data. Radiocarbon 19, 355-363.

Thomsen, K.J., Murray, A.S., Jain, M., Bøtter-Jensen, L., 2008. Laboratory fading rates of various luminescence signals from feldspar-rich sediment extracts. Radiation measurements 43, 1474-1486.

Thomsen, K.J., Murray, A.S., Jain, M., 2012. The dose dependency of the overdispersion of quartz OSL single grain dose distributions. Radiation Measurements 47, 732-739.

Tissoux, H., Falguères, C., Voinchet, P., Toyoda, S., Bahain, J.-J., Despriée, J., 2007. Potential use of Ti-center in ESR dating of fluvial sediment. Quaternary Geochronology 2, 367-372.

Tissoux, H., 2015. Sediment, ESR. Encyclopedia of Scientific Dating Methods. J. W. Rink and J. Thompson. Dordrecht, Springer Netherlands, 743-747.

Torfstein, A., Goldstein, S.L., Kagan, E J., Stein, M., 2013. Integrated multi-site U-Th chronology of the last glacial Lake Lisan. Geochimica et Cosmochimica Acta 104, 210-231.

Toyoda, S., Voinchet, P., Falguères, C., Dolo, J.M., Laurent, M., 2000. Bleaching of ESR signals by the sunlight: a laboratory experiment for establishing the ESR dating of sediments. Applied Radiation and Isotopes 52, 1357-1362.

Toyoda, S., 2015. Paramagnetic lattice defects in quartz for applications to ESR dating. Quaternary Geochronology 30, 498-505.

Turney, C.S., Coope, G.R., Harkness, D.D., Lowe, J.J., Walker, M.J., 2000. Implications for the dating of Wisconsinan (Weichselian) Late-Glacial events of systematic radiocarbon age differences between terrestrial plant macrofossils from a site in SW Ireland. Quaternary Research 53, 114-121.

Vandenberghe, J., Gracheva, R., Sorokin, A., 2010. Postglacial floodplain development and Mesolithic-Neolithic occupation in the Russian forest zone. Proceedings of the Geologists' Association 121, 229–237.

van der Schriek, T., Passmore, D.G., Franco Mugica, F., Stevenson, A.C., Boomer, I., Rolao, J., 2008. Holocene palaeoecology and floodplain evolution of the Muge tributary, Lower Tagus Basin, Portugal. Quaternary International 189, 135–151.

Van Der Woerd, J., Ryerson, F.J., Tapponnier, P., Gaudemer, Y., Finkel, R., Meriaux, A.S., Caffee, M., 1998. Holocene left-slip rate determined by cosmogenic surface dating on the Xidatan segment of the K'unlun fault (Qinghai, China). Geology 26, 695–698.

Veldkamp, A., Kroonenberg, S., Heijnis, H., Ven den Berg van Saparoea, R., 2004. The suitability of dated travertines as a record of fluvial incision: Allier (France) floodplain dynamics during the late Quaternary. Quaternaire 15, 159–165.

Vis, G.J., Kasse, C., Kroon, D., Jung, S., Zuur, H., Prick, A., 2010. Late Holocene sedimentary changes in floodplain and shelf environments of the Tagus River (Portugal). Proceedings of the Geologists' Association 121, 203–217.

Voinchet, P., Bahain, J.J., Falguères, C., Laurent, M., Dolo, J.M., Despriée, J., Gageonnet, R., Chaussé, C., 2004. ESR dating of quartz extracted from Quaternary sediments application to fluvial terraces system of northern France. Quaternaire 15, 135–141.

Voinchet, P., Falguères, C., Tissoux, H., Bahain, J.-J., Despriée, J., Pirouelle, F., 2007. ESR dating of fluvial quartz: Estimate of the minimal distance transport required for getting a maximum optical bleaching. Quaternary Geochronology 2, 363-366.

Voinchet, P., Toyoda, S., Falguères, C., Hernandez, M., Tissoux, H., Moreno, D., Bahain, J.J., 2015. Evaluation of ESR residual dose in quartz modern samples, an investigation on environmental dependence. Quaternary Geochronology 30, 506-512.

Wallinga, J., 2002. Optically stimulated luminescence dating of fluvial deposits: a review. Boreas 31, 303-322.

Wallinga, J., Murray, A.S., Duller, G.A., Törnqvist, T.E., 2001. Testing optically stimulated luminescence dating of sand-sized quartz and feldspar from fluvial deposits. Earth and Planetary Science Letters 193, 617-630.

Wang, X.L., Lu, Y.C., Wintle, A.G., 2006. Recuperated OSL dating of fine-grained quartz in Chinese loess. Quaternary Geochronology 1, 89-100.

Wang, X., Van Balen, R., Yi, S., Vandenberghe, J., Lu, H., 2014. Differential tectonic movements in the confluence area of the Huang Shui and Huang He rivers (Yellow River), NE Tibetan Plateau, as inferred from fluvial terrace positions. Boreas 43, 469–484.

Wedepohl, H.K., 1995. The composition of the continental crust. Geochimica et Cosmochimica Acta 59, 1217-1232.

Wenz, S., Scholz, D., Sürmelihindi, G., Passchier, C.W., Jochum, K.P., Andreae, M.O., 2016. ^{230}Th/U-dating of carbonate deposits from ancient aqueducts. Quaternary Geochronology 32, 40-52.

Wintle, A.G., 1973. Anomalous fading of thermoluminescence in mineral samples. Nature 245, 143-144.

Wintle A.G., Murray, A.S., 2006. A review of quartz optically stimulated luminescence characteristics and their relevance in single-aliquot regeneration dating protocols. Radiation Measurements 41, 369-391.

Wolf, D., Seim, A., Faust, D., 2014. Fluvial system response to external forcing and human impact - Late Pleistocene and Holocene fluvial dynamics of the lower Guadalete River in western Andalucía (Spain). Boreas 43, 422–449.

Yang, Q., Scholz, D., Jochum, K.P., Hoffmann, D.L., Stoll, B., Weis, U., Schwager, B., Andreae, M.O., 2015. Lead isotope variability in speleothems - A promising new proxy for hydrological change? First results from a stalagmite from western Germany. Chemical Geology 396, 143-151.

Zermano, P., Kurdyla, D.K., Buchoilz, B.A., Heller, S.J., Kashgarian, M. Frantz, B.R., 2004. Prevention and removal of elevated radiocarbon contamination in the LLNL/CAMS natural radiocarbon sample preparation laboratory. Nuclear Instruments and Methods in Physics Research B 223–224, 293–297.

Zielhofer, C., Faust, D., 2008. Mid- and Late-Holocene fluvial chronology of Tunisia. Quaternary Science Reviews 27, 580-588.

Zhu, S., Wu, Z., Zhao, X., Li, J., Xiao, K., 2014. Ages and genesis of terrace flights in the middle reaches of the Yarlung Zangbo River, Tibetan Plateau, China. Boreas 43, 485–504.

Table captions

Table 1. Case studies published in outcomes relative to former FLAG activities using one (or more) numerical dating methods detailed in the text.

FLAG special	**Radiocarbon**	**Luminescence**	**ESR**	**^{230}Th/U**	**TCN**
Quaternaire 15, Issue 1-2 (2004)	Briant et al.;		Chaussé et al.;		
	Flez and	Jain et al.	Despriée et	Veldkamp et al.	
	Salvador et al.	Mol et al.	Voinchet et al.		
	Kuzucuoglu et al.				
	Mathieu et al.				
Quaternary International 189, Issue 1 (2008)	Fontana et al.				
	Kalicki et al.				
	van der Schriek et				
Geomorphology 98, Issue 3-4 (2008)	de Moor et al.				
Proceedings of the Geologists' Association, 121, Issue 2 (2010)	Coltorti et al.	Lauer et al.			
	Kasse et al.	Martins et al.			
	Vandenberghe et				
	Vis et al.				
Geomorphology, 165-166 (2012)		Cordier et al.			Antón et al.
		Cunha et al.			
		Ramos et al.			
Géomorphologie, Relief, Processus, Environnement, Issue 4 (2012)	Le Jeune et al.				
	Piovan et al.				
Boreas 43, Issue 2 (2014)	Wolf et al.	Cordier et al.	Zhu et al.		Rixhon et al.
	Zhu et al.	Wang et al.			
Quaternaire 26, Issue 1 (2015)	Garnier et al.		Harmand et al.		

1521 Table 2. Sampling and laboratory techniques to improve accuracy in radiocarbon dating fluvial

1522 deposits. AMS = accelerator mass spectrometry.

Issue	Sampling/laboratory solution
1) Dating suitable material	
Age difference between ^{14}C dated sediment deposit and the deposit / event for which an age is required	Select samples for dating according to sedimentary context and, where possible, from close to boundaries between sedimentary units (c.f. 'change after' dates (Macklin et al., 2010).
Danger of reworking of fossil material either whole or as organic detritus (e.g. Rogerson et al., 1992)	Date only the identifiable fraction of the deposit – e.g. thoroughly cleaned specific plant macrofossils, shells or bones (e.g. Turney et al., 2000). This is only possible because of AMS techniques which allow dating of small samples.
Danger of field contamination by modern organic detritus	
2) Freshwater reservoir effect	
Danger of carbon uptake from carbonate rich water rich in 'old' carbon	Date only macrofossils from terrestrial species which do not photosynthesise under water (e.g. Carex, Scirpus).
3) Pretreatments to remove contaminants	
Danger of secondary carbonate from post-depositional groundwater infiltration	Dilute HCl pre-treatment (first step of the mild ABA below).
Danger of humic acid infiltration from higher in the profile – especially if overlain by peat	For younger samples (< ~25 ^{14}C yr BP): mild acid-base-acid (ABA) washes as standard pretreatment For older samples, other pretreatments are recommended to remove more contamination: • Ultrafiltration on bone (e.g. Higham et al., 2006) • ABOx-SC (acid, base, wet oxidation - stepped combustion) on charcoal (Bird et al., 1999) • No clear favoured protocols as yet for seeds or shells
4) General considerations	
Sampling and laboratory preparation.	• Ensure laboratory space and all equipment being used for preparation has never previously come into contact with radioactive elements (e.g. from biological researchers using ^{14}C as a tracer element – Zermeno et al., 2004). • Avoid organic packaging such as paper • Process and store sample in deionised water only • Clean working conditions, avoiding contact of samples or equipment with paper where possible • Powderless laboratory gloves • Visual checks for contamination • Dry samples soon after identification to prevent fungal growth during storage • Submit as large a sample size as possible – preferably >1.4 mg carbon content, i.e. >5 mg dry weight (Brock et al., 2010)

1523

1524

1525 Table 3. A brief overview of the OSL dating method applied to quartz and feldspar grains extracted
1526 from sediment.

	Quartz (SAR)	Quartz (TT-OSL)	Feldspar (IRSL)	Feldspar (pIR-IRSL)
Upper dating range	Present-day			
Lower dating range	200-300 Gy – i.e. c. 150 ka + (depending on dose rate)	c. 950 ka	Unclear due to anomalous fading – c. 300 ka?	c. 950 ka
Main strength of the application	Can date fluvial sediments directly. Can date beyond the C-14 dating time range. TT-OSL and pIR-IRSL can extend back to c. 1 Ma			
Standard precision	Standard errors are usually ~10% (5-15%)			

1527

1528

1529

1530 Table 4. A brief overview of the ESR dating method applied to fossil teeth and optically bleached
1531 quartz grains extracted from sediment. Further details regarding the dating time range of each
1532 application may be found in Duval (2016) and references therein.

	Fossil tooth enamel	Optically bleached quartz grains extracted from sediment
Dated event	Burial of the fossil tooth (usually assumed to happen shortly after the death of the animal).	Last exposure of the sediment to sunlight
Main specificity of the application	Dental tissues are open-systems for U: U-uptake needs to be modeled (combined U-Series/ESR dating approach).	Light-sensitive ESR signals (same basic principles as OSL dating). Presence of a residual (non-bleachable) ESR intensity for the Al centre.
Upper dating range	Present-day	~10 ka
Lower dating range	Early Pleistocene	Miocene (Al-center)
Optimum dating range	40-800 ka	200 ka-2 Ma
Main strength of the application	Direct dating of hominin and animal fossil remains beyond the C-14 and U-series dating time range.	May date beyond the OSL dating time range.
Standard precision	Standard errors are usually ~10% (5-15%)	Standard errors are usually ~10% (5-15%)

1533

1534

1535

1536

Table 5. Summary of the main features usually observed for the three paramagnetic centres Al, Ti-Li and Ti-H. Relative characterisation is provided: (+++)=high, (++)=medium, (+)=low. Further details and additional references may be found in the text.

	Al Centre	***Ti-Li Centre***	***Ti-H Centre***
Signal-to-Noise ratio (S/N)	+++	++	+
Precision of the measurements	+++	++	+
Dose response curve	*No apparent saturation at high doses (>60 kGy)*	*Non-monotonic behaviour (maximum intensity ~6-10 kGy)*	*Non-monotonic behaviour (maximum intensity ~3-8 kGy)*
Bleaching kinetics (speed)	+	++	+++
Residual ESR intensity (unbleachable component)	*Yes*	*No*	*No*

Figure captions

Fig. 1. Dateable ranges of the five numerical dating methods detailed in this contribution. Black rectangles refer to time spans within which the methods usually provide reliable results; dashed rectangles represent challenging time periods. Luminescence methods are divided into two rows: the first row represents the routinely applied techniques (OSL: optically stimulated; IRSL: infrared stimulated, including pIRIR) and the second row the techniques currently under development (TT: thermally transferred; RF: radiofluorescence). ESR dating on quartz and U-series/ESR dating of tooth enamel as well as surface exposure dating and burial dating with terrestrial cosmogenic nuclides (TCN) are also divided because of the different dating principles.

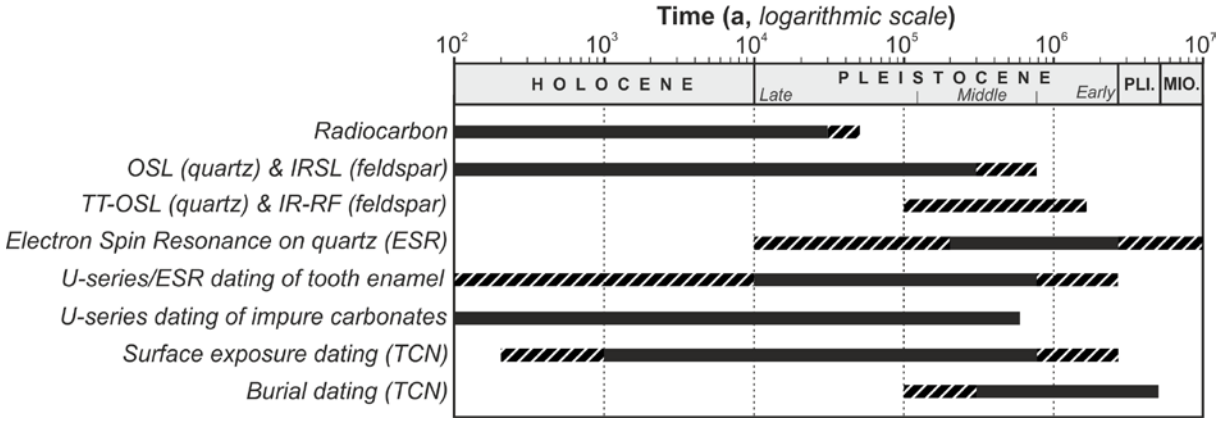

Fig. 2. Sketch representing the dateable deposits/landforms and the pathways of dateable material for ^{14}C, OSL/IRSL, ESR, $^{230}Th/U$ and TCN dating in both braided and meandering fluvial systems. Transport pathways and temporary storages of both inorganic (gravel, sand, silt) and organic (bone, charcoal, opercula, seed, shell and tooth) materials on hillslopes and in the fluvial system are also represented.

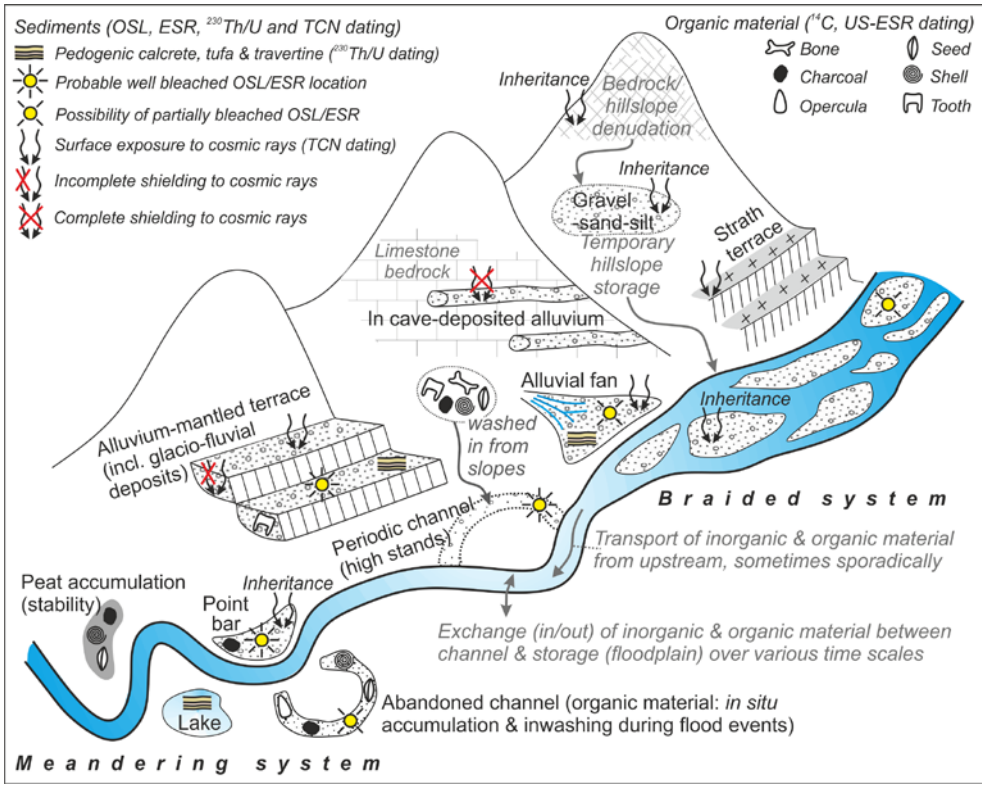

Fig. 3. The impact of modern contamination (0.25–2% by weight) on measured ^{14}C ages (thin lines) compared to the 1:1 or uncontaminated line (thickest line). After Pigati et al. (2007)

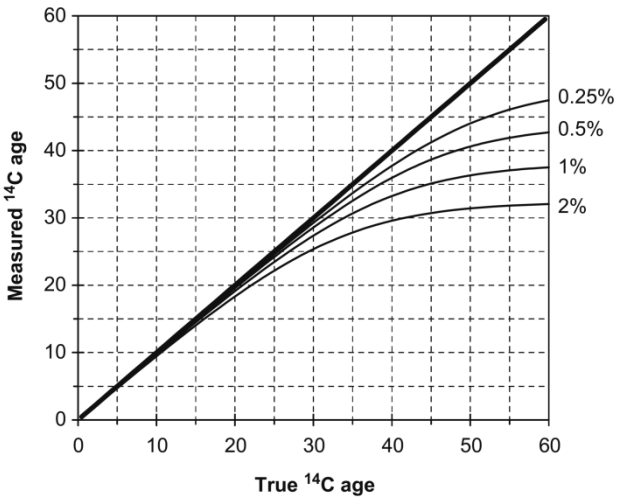

Fig. 4. a) A good sampling location for Luminescence dating at Stanswood Bay, Hampshire, England (Briant et al., 2006). The thickest sand bed at the base is Mesozoic in age, but samples were taken from thick sand beds above the gravel channel (as shown and above the photo out of view). b) Less optimal sampling location for Luminescence dating at Barton on Sea, Hampshire, England (Briant et al., 2006). Field gamma spectrometry was undertaken to mitigate the complex dose rate effect of the thinner sand lenses.

Fig. 5. Comparison of two common methods of plotting data (82 aliquots of aeolian quartz). The radial plot on the right is able to show both precision and equivalent dose on the same plot. This is not possible with the histogram on the left, nor with commonly used probability density plots. Figures 1 and 2 of Galbraith (2010).

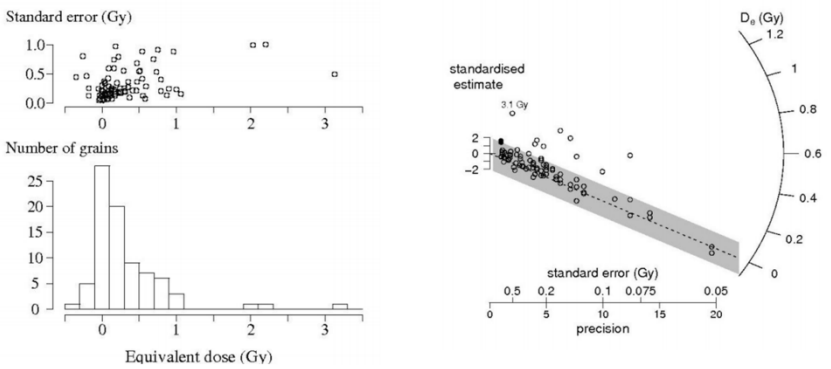

Fig. 6. a) Examples of ESR spectra of Al and Ti centres measured in quartz. b) Decay of the ESR intensity of the different centres Al, Ti-Li and Ti-H under UV exposure. This laboratory bleaching experiment was performed with a SOL2 sunlight simulator (Dr Hönle) on a quartz sample from the Morée-Villeprovert locality, France.

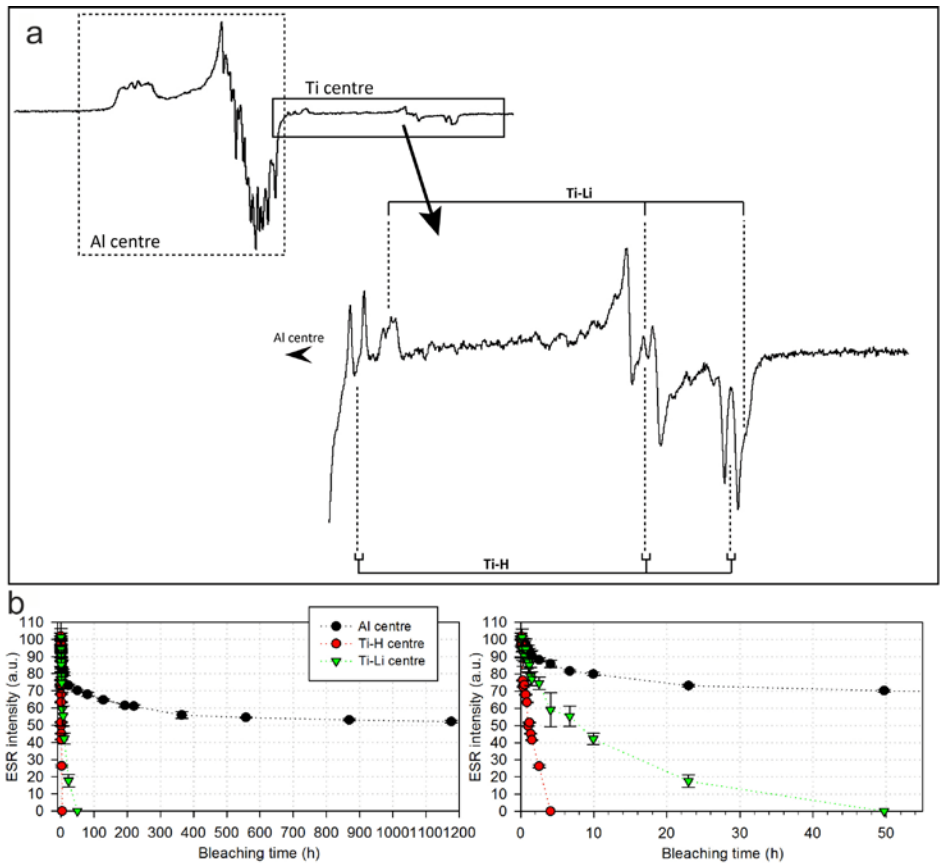

Fig. 7. Surface exposure dating: application of distinct sampling strategies to different fluvial archives or landforms (left), exemplified by dating results (right). a) Sandstone boulder lying at the surface of an alluvial fan, sampled for ^{10}Be concentration measurement (Escondida creek, Andean Precordillera, Argentina). After Schmidt et al. (2011); b) Mean surface exposure ages (bold numbers), calculated from ^{10}Be and ^{26}Al concentration measurements in individual clasts samples, for three fan terraces displaced by Holocene strike-slip faulting activity (NE Tibet). The young age cluster on T1 is attributed to the occurrence of a recent flash flood (light arrow) whereas the four samples from T1, T2 and T3 with much older apparent ages (dark arrows) are supposed to have been reworked from older deposits but may also have a higher inherited content. After Van der Woerd et al.(1998); c) Sketch of TCN concentrations along a depth profile (bold black curve) in an alluvial sequence deposited in a

single event, highlighting a concentration decrease with depth. Red curves represent supposed frequency distribution of nuclide concentrations of individual clasts, illustrating the need to amalgamate tens of clasts. Modified after Ivy-Ochs and Kober (2008); d) measured ^{10}Be concentrations with 1σ error bars along a ~4.5 m-deep profile in terrace sediments (Ourthe river, Ardenne massif, Belgium) and modelled curves based on 10 or 9 samples (bold and dashed curves, respectively). Modified after Rixhon et al. (2011); e) two distinct levels of fluvially-carved strath terraces; both bedrock surfaces were sampled for ^{10}Be concentration measurements (Susquehanna river, Appalachian mountains, USA). After Reusser et al. (2004); f) Sketch summarizing the Late Pleistocene incision in the Susquehanna river based on ^{10}Be concentrations of distinct strath terraces (with a minimum age for the upper, strongly eroded surface); g) Normalized cumulative probability curves based on the sample numbers of fig. f for the three lower terrace levels. After Reusser et al. (2006).

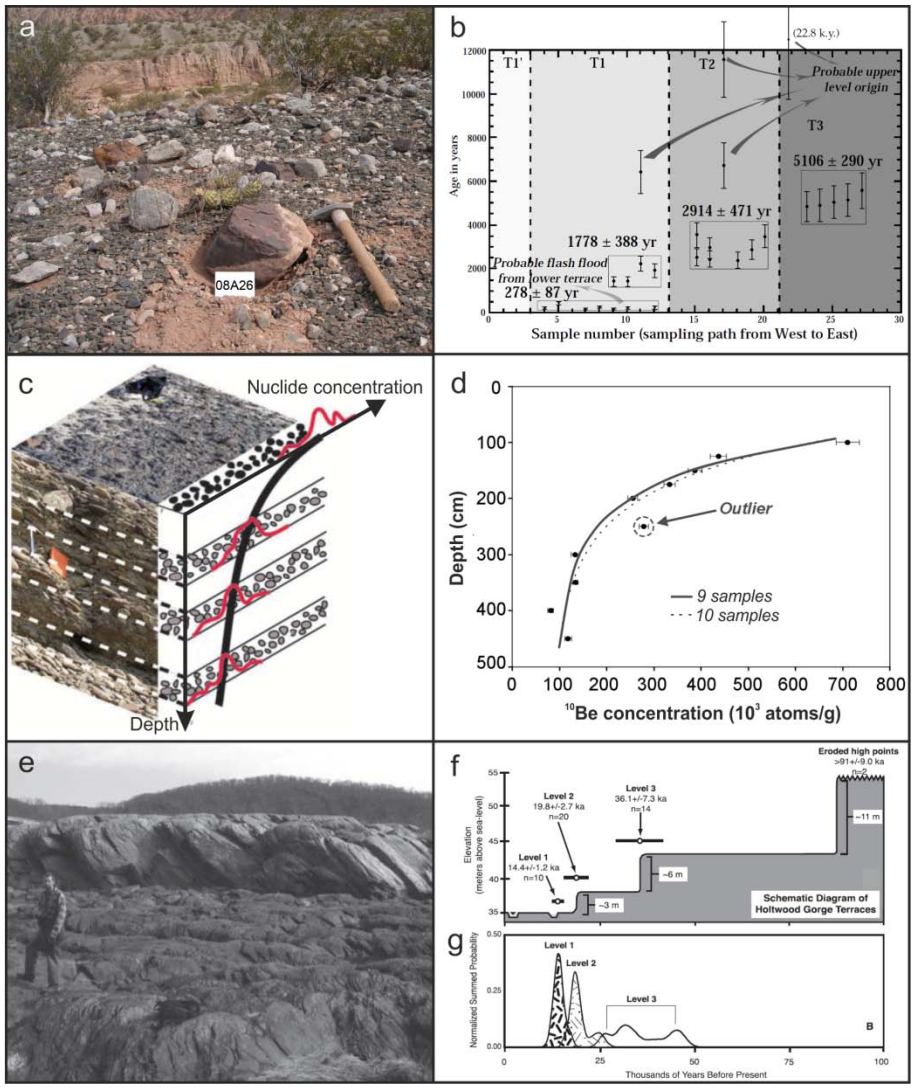

Fig. 8. Burial dating: application of two sampling strategies to different fluvial archives (left), exemplified by dating results (right). a) Horizontal, abandoned phreatic tube, partly filled with river sediments (Cumberland river catchment, Appalachian mountains, USA). Note the regular elliptic cross-section of the former phreatic passage. After Anthony and Granger (2007), photo: D. Granger; b) Topographic cross-section across the South Fork river canyon (Sierra Nevada, USA) displaying the multi-level cave system in which burial dating was performed. Note the significant decrease of incision rates toward present. After Stock et al. (2004); c) erosion-burial diagram, the bold line represents the $^{26}Al/^{10}Be$ ratio in steadily eroding rocks whereas the dashed curves refer to equal burial duration (dotted lines refer to pre-burial erosion rates). All samples plot beneath the bold line and have therefore experienced burial (New river, Appalachian mountains, USA). After Granger et al. (1997); d) ~10 m-thick, gravel terrace body overlain by a tephra layer, sampled at the base for isochron burial dating because of insufficient shielding to cosmic rays (Gunnison river, Colorado plateau, USA). After Darling et al. (2013), photo: L. Crossey; e) Graphical representation of burial dating isochron for a gravel terrace, the burial age is calculated from the slope of the regression line (Sundays river, South Africa). After Erlanger et al. (2012).

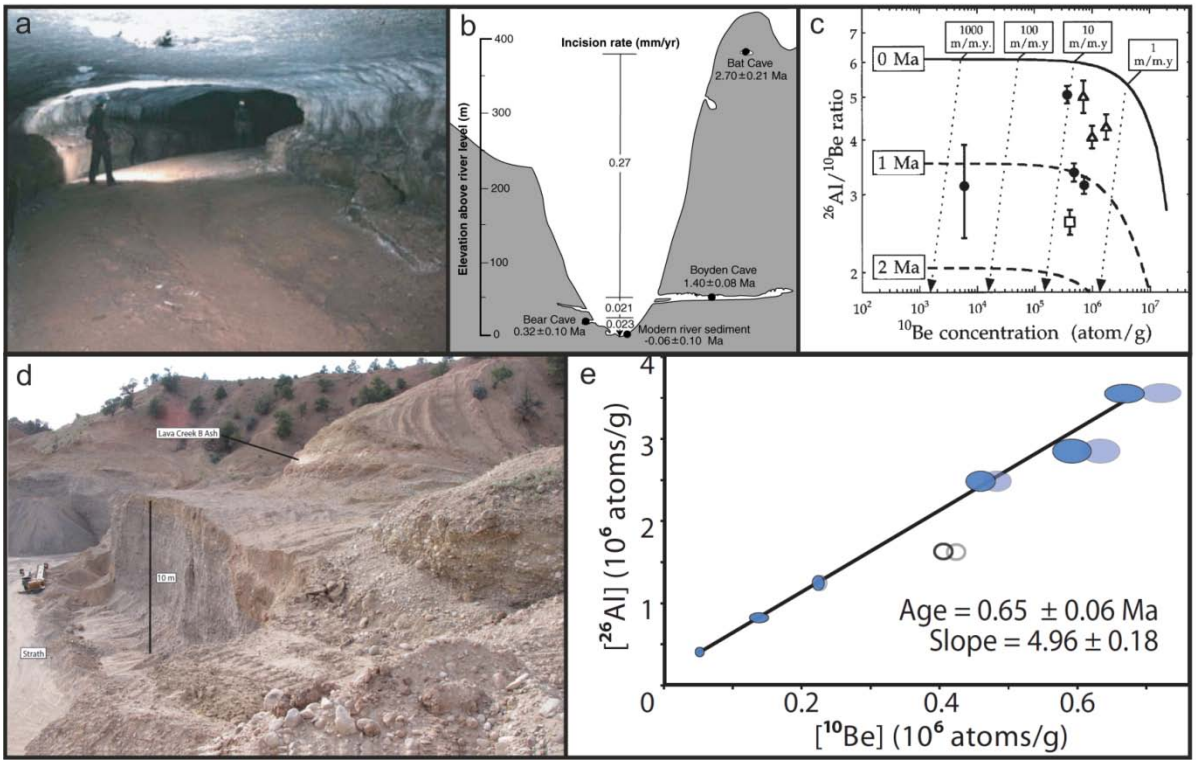

Fig. 9. a) Comparison of ^{14}C (uncertainties: one standard deviation) and OSL (uncertainties: one standard error) dates. Calibration of radiocarbon dates: Calib 5.0 (Stuiver et al., 2005) with the IntCal04 dataset (Reimer et al., 2004) for ages <26 ^{14}C ka BP and Fairbanks et al. (2005) for ages >26 ^{14}C ka BP. Note the systematic age underestimation of ^{14}C dating beyond the 29-35 ka limit. After Briant and Bateman (2009). b) Plot showing ^{10}Be depth profile ages and $^{230}Th/U$ ages for alluvial fan deposits, both with 2σ error. Shaded red and blue boxes represent the mean ^{10}Be exposure age and mean U-series age, respectively. Note the slightly younger age range of $^{230}Th/U$ dating (minimum age) than the one defined by the depth profile, proving the usefulness of this combined approach. After Blisniuk et al. (2012). c, d) Integrated ^{10}Be depth profile and OSL model results in the model parameter space of deposition time (t_1), exposure time (t_2), and ^{10}Be inheritance for a single alluvial sequence. The cosmogenic nuclide model best fit (thick red dot) with the 68% confidence level envelope around it (red surface), the OSL model best fit (vertical blue line) with the 68% confidence level envelope around it (blue surface) and the intersection of the two confidence surfaces (dark surface) are shown on (c). The intersection alone is represented on (d), with its 2D projection onto the axial planes (grey surfaces) and further 1D reprojection onto the axes (grey labelled lines). After Guralnik et al. (2011).